Copyright Warning & Restrictions

The copyright law of the United States (Title 17, United States Code) governs the making of photocopies or other reproductions of copyrighted material.

Under certain conditions specified in the law, libraries and archives are authorized to furnish a photocopy or other reproduction. One of these specified conditions is that the photocopy or reproduction is not to be "used for any purpose other than private study, scholarship, or research." If a, user makes a request for, or later uses, a photocopy or reproduction for purposes in excess of "fair use" that user may be liable for copyright infringement,

This institution reserves the right to refuse to accept a copying order if, in its judgment, fulfillment of the order would involve violation of copyright law.

Please Note: The author retains the copyright while the New Jersey Institute of Technology reserves the right to distribute this thesis or dissertation

Printing note: If you do not wish to print this page, then select "Pages from: first page # to: last page #" on the print dialog screen

Abstract

Name: Amer Muhammad Alsawadi

Advisor: Dr. Edip Niver

Thesis Title: Wideband Microstrip Antenna Optimization

An annular ring patch microstrip antenna was investigated numerically from the bandwidth aspect for a satellite link application. The desired portable antenna should occupy the physical volume of a typical briefcase and operate in the 400-500 MHz band. Numerical optimization is carried out using a commercially available computer package (EM, by Sonnet Software Inc.). The parameters optimized include the substrate thickness, feed location along the annular patch antenna and its relative dimensions. The software package was numerically validated for the rectangular patch geometries reported in the open literature. Experimental verification of this work is left to be carried out in the near future.

2) WIDEBAND MICROSTRIP ANTENNA OPTIMIZATION

by

1) Amer Muhammad Alsawadi

Thesis

Submitted to the Faculty of the Graduate Division of

New Jersey Institute of Technology

in Partial Fulfillment of the Requirements for the Degree of

Masters of Science

Department of Electrical Engineering

Dec. 1990

APPROVAL SHEET

Title of Thesis: Wideband Microstrip Antenna Optimization

Name of Candidate: Amer Muhammad Alsawadi

Master of Science in Electrical Engineering, 1990

Thesis and Abstract Approved: _____ _____

Dr. Edip Niver Date

Associate Professor

Department of Electrical Engineering

_____ _____

Dr. Gerald Whitman Date

Professor

Department of Electrical Engineering

_____ _____

Dr.Erdal Panayirci Date

Visiting Professor

Department of Electrical Engineering

Vita

Author: Amer Muhammad Alsawadi

Degree: Master of Science in Electrical Engineering

Date: Dec. 1990

Undergraduate and Graduate Education:

- Master of Science in Electrical Engineering, New Jersey Institute of Technology, Newark, NJ, 1990
- Bachelor of Science in Electrical Engineering, King Fahd University of Petroleum and Minerals, Dhahran, Saudi Arabia, 1989

Major: Electrical Engineering

ACKNOWLEDGMENT

The author wiches to express his sincere gratitude to his advisor Dr. Edip Niver for his guidance, support, friendship and trust through the entire period of study.

TABLE OF CONTENTS

LIST OF TABLES

LIST OF FIGURES

Chapter I

WIDEBAND MICROSTRIP ANTENNA FOR A SATELLITE LINK

Introduction

A microstrip line consists of a metallic strip supported by a dielectric substrate over a conducting ground plane. Such a structure is found in various applications as a transmission line because of its low loss, low cost and ease of fabrication using printed circuit techniques. Further applications involve various components where microstrip lines are used to realize filters, couplers and other passive functions. The idea of using a microstrip to construct antennas had lead to various developments [2,4,6]. Microstrip antennas have gained considerable popularity in recent years mainly due to the antenna assembly being physically very small, flat and inexpensive [7,2]. Sometimes these antennas are called printed antennas because of the manufacturing process [2]. Although there are many kinds of microstrip antennas, common features among all of them include

- a very thin flat metallic region called the patch,
- a dielectric substrate,
- a flat metallic region usually much larger than the patch called the ground plane,
- a feed structure which excites the patch.

A typical example of a microstrip antenna is shown in Figure 1. The patch can have any shape such as rectangular, circular, etc,. There exists an extensive literature on microstrip antennas and still more being published on the analysis and synthesis aspects in new

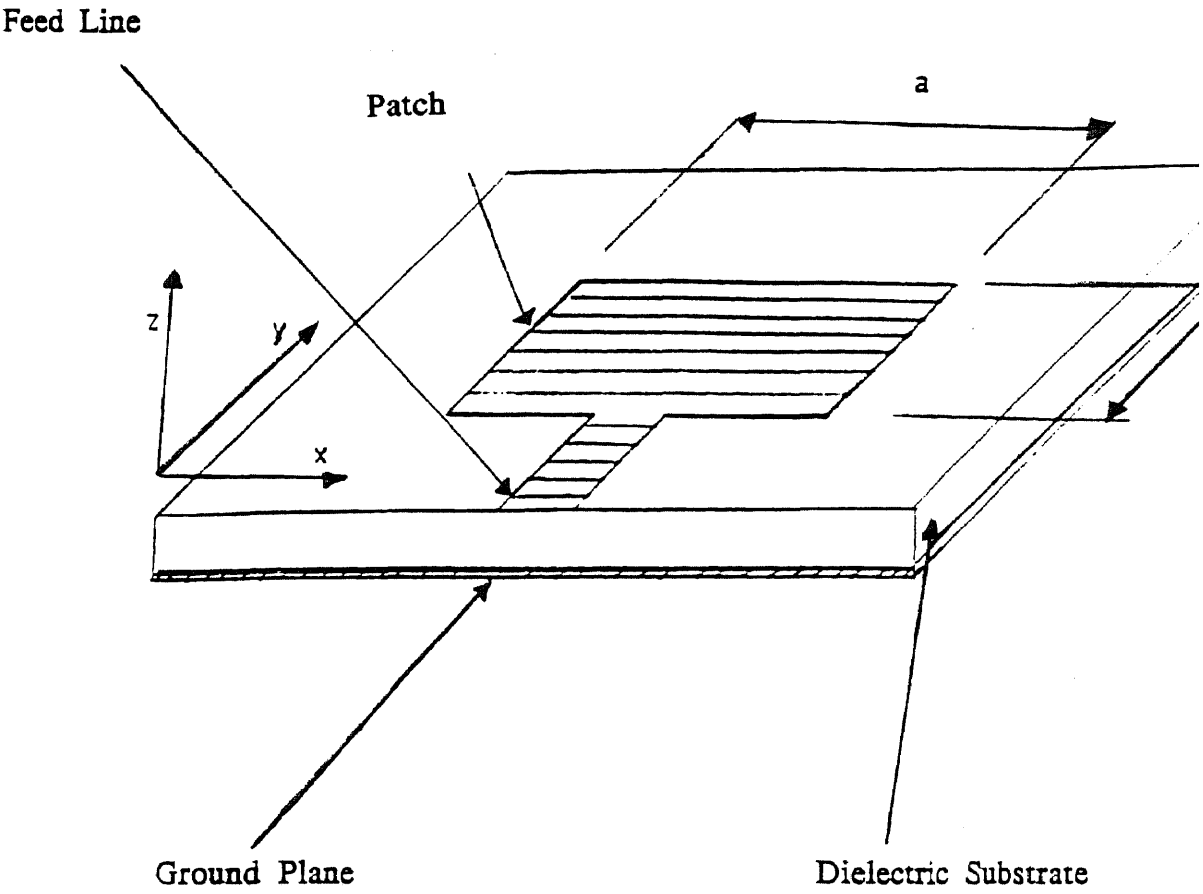

Figure 1. A typical example of microstrip antennas.

applications. The advantages of microstrip antennas are [4] :

- light weight, low volume, low profile,
- low fabrication cost,
- ease of mounting on missiles, rocket, satellites and other supporting structures,
- linear (LP), circular (RHCP or LHCP) polarizations are achievable,
- dual frequency operation is possible,
- no cavity packing required,
- they are physically compatible to solid state devices such as oscillators, amplifiers, variable attenuators, switches, modulators, mixers, phase shifters, etc, and these can be added directly to the antenna substrate board,
- feed lines and matching networks are fabricated simultaneously with the antenna structure.

However, with all of these advantages microstrip antennas have some disadvantages compared to conventional microwave antennas,which are [4] :

- narrow bandwidth,
- low gain,
- half plane radiation,
- practical limitations on the maximum gain (about 20 db),
- poor endfire radiation performance,
- poor isolation between feed and radiating elements,
- possibility of excitation of surface waves,

– lower power handling capability,

For many practical designs, the advantages of these antennas far outweigh their disadvantages. The application areas for such antennas are in satellite communication, radar, radio altimeter, command and control, missile telemetry, weapon fusing, manpack equipment, environmental instrumentation and remote sensing, feed elements in complex antennas, satellite navigation receivers, biomedical radiators, etc.. The analysis and design of the microstrip antenna presented here has a possible application as a portable antenna operated on the ground for a satellite link.

Problem Description

The portable satellite antenna that is available in the 400-500 MHz band is an ordinary folded dipole antenna which can be compacted into a small size. However, for field operation it has to be deployed and then its dimensions span (typically 73 cm long, 73 cm wide, and 33 cm high). The time that it requires for deployment and connection to the system and the large size could be an obstacle for an efficient operation. A microstrip antenna that fits into a briefcase or a part of the briefcase was suggested as an alternative. The antenna can be put on one side of the briefcase and the rest of the system could occupy the remaining part. Hence, the ultimate solution is when the user opens the briefcase, the system is ready for operation.

Typical required specifications to be met are :

– Bandwidth ($\sim$ 100 Mhz),

- Operation frequency (~ 450 Mhz),
- Circular polarization,
- Fits into a briefcase (Height ~ 13cm, Width ~ 45cm, Length ~ 55cm).

Typical constraints encountered in this work are as follows. Available computer packages provided us with bandwidth information. However, polarization of the radiated field has to be determined because the existing package is limited to scattering parameters defined at the input ports. Currently, there is no access to the current distribution evaluated within this package.

Suggested Solution

Objectives for this antenna design are mainly

1)to achieve the range of frequency for satellite communication with the antenna size not to exceed that of a briefcase,

2)to satisfy the required wide bandwidth and

3)to obtain radiation with circular polarization.

This work attempts to fulfill the above goals by optimizing the patch geometry, thickness of the substrate(s), dielectric constant and selection of the proper feed location(s).

Chapter II

THEORY

Radiation Mechanism of Microstrip Antennas

To understand the radiation mechanism of a microstrip antenna [2], consider a rectangular microstrip patch spaced a small fraction of a wavelength above a ground plane, as shown in Figure 2. The electric field along the conducting patch shows no variation. However, fringing fields in the region surrounding the patch are the primary sources for radiation. These surrounding fields on each side can be resolved into normal and tangential components with respect to the ground plane. For a half-wavelength patch as shown in Figure 3, the normal components of the fringing fields are out of phase by 180 degrees and hence their contributions to radiation tends to cancel out. However, the tangential components are in phase and contribute collectively, to produce maximum radiated field normal to the surface of the structure. Now, the patch can be represented by two equivalent parallel slots half of a wavelength apart, excited in phase and radiating into the half-space above the ground plane as shown in Figure 4. Taking into consideration the variation of fields along the width of the patch, we can represent the antenna by four slots, and hence by four equivalent current distributions, surrounding the patch structure. Similarly, this approach can be extended to other microstrip antenna configurations [2].

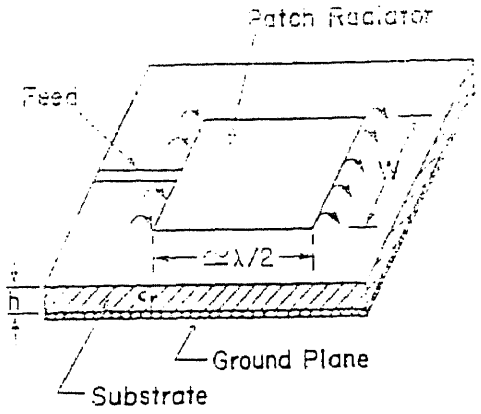

Figure 2. A rectangular microstrip patch spaced a fraction of a wavelength above the ground plane.

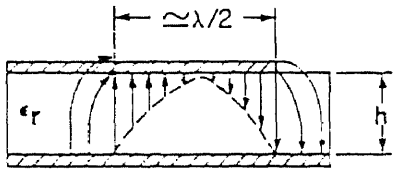

Figure 3. Electric field configuration of the radiator.

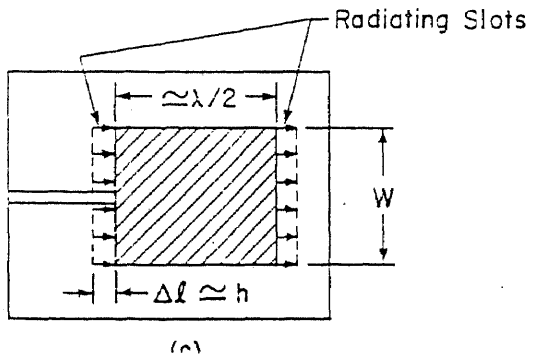

Figure 4. Two slots representation of the patch.

Radiation Fields

After neglecting any radiation from the feed lines, it can be shown that the major contributions to the far-zone fields are due to the equivalent electric and magnetic surface currents produced by fringing fields which lie on a closed surface surrounding the antenna. The equivalent electric surface current density $\bar{K}$ is defined as

$$\bar{K} = \hat{n} \times \bar{H} \tag{1}$$

and the equivalent magnetic surface current density $\bar{M}$ is given by

$$\bar{M} = \bar{E} \times \hat{n} \tag{2}$$

where $\hat{n}$ is an outward normal unit vector to the surface and $\bar{E}$ and $\bar{H}$ are the electric and magnetic field density vectors in the surrounding region.

The principle of superposition can be used to represent contribution at any field point $\bar{r}$ away from the source region, due to electric and magnetic current distributions. The fields produced by the electric current distribution are

$$\bar{E}^e(r) = \left[\frac{-j}{\omega\mu\varepsilon}\right] \nabla (\nabla \cdot \bar{A}) - j\omega\bar{A} \tag{3}$$

$$\bar{H}^e(r) = \left[\frac{1}{\mu}\right] \nabla \times \bar{A} \tag{4}$$

where ε and μ are the medium parameters. These parameters (ε,μ) may either represent the substrate or the medium surrounding the antenna, which is (ε_o,μ_o) for free space. The superscript e indicates the electric nature of resulting fields due to an electric current distribution. Here, the magnetic vector potential is given as

$$\bar{A} = \left[\frac{\mu}{4\pi}\right] \iint_s \bar{K}(\bar{r}') \frac{e^{-jk_o|\bar{r} - \bar{r}'|}}{|\bar{r} - \bar{r}'|} ds' \quad (5)$$

where the free space wavenumber $k_o = \omega\sqrt{\varepsilon_o\mu_o}$ and ω is the angular frequency. The prime coordinates indicate the source location as shown in Figure 5. Similarly, fields due to magnetic currents are denoted by the superscript m and are given by

$$\bar{E}^m(r) = \left[\frac{-1}{\varepsilon}\right] \nabla \times \bar{F} \quad (6)$$

$$\bar{H}^m(r) = \left[\frac{-j}{\omega\mu\varepsilon}\right] \nabla (\nabla \cdot \bar{F}) - j\omega\bar{F} \quad (7)$$

where

$$\bar{F} = \left[\frac{\varepsilon}{4\pi}\right] \iint_s \bar{M} (\bar{r}') \frac{e^{-jk_o|\bar{r} - \bar{r}'|}}{|\bar{r} - \bar{r}'|} ds' \quad (8)$$

The combined fields after applying the principle of superposition are

$$\bar{E} (r) = \bar{E}^e + \bar{E}^m = \left[\frac{-j}{\omega\mu\varepsilon}\right] \nabla (\nabla \cdot \bar{A}) - j\omega\bar{A} - \left[\frac{1}{\varepsilon}\right] \nabla \times \bar{F} \quad (9)$$

and

$$\bar{H} (r) = \bar{H}^e + \bar{H}^m = \left[\frac{1}{\mu}\right] \nabla \times \bar{A} - \left[\frac{j}{\omega\mu\varepsilon}\right] \nabla (\nabla \cdot \bar{F}) - j\omega\bar{F} \quad (10)$$

Both magnetic and vector potentials are solutions to the following wave equations

$$\nabla^2 \bar{A} + \omega^2\mu\varepsilon \bar{A} = 0 \quad (11)$$

$$\nabla^2 \bar{F} + \omega^2\mu\varepsilon \bar{F} = 0 \quad (12)$$

In the far zone, the only significant components are those which are

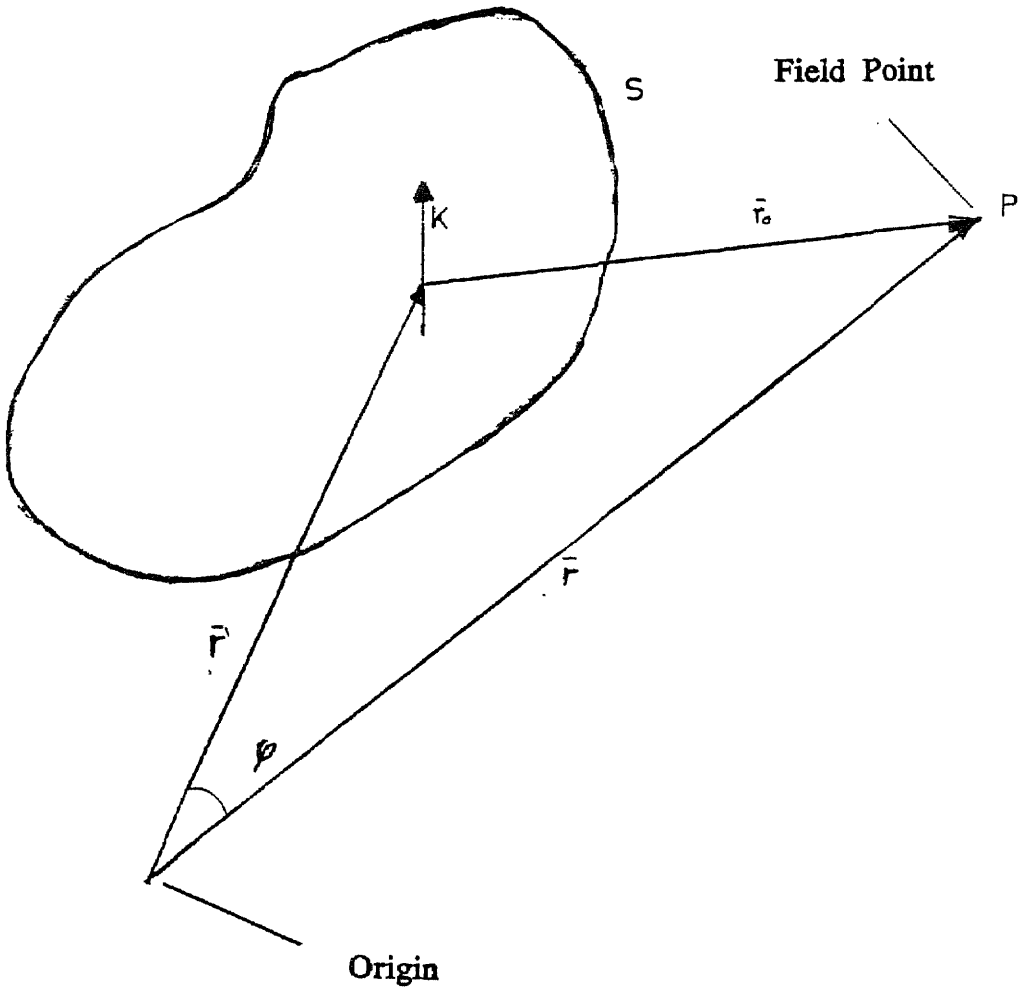

Figure 5. Coordinates for a microstrip patch antenna

transverse to the direction of propagation. Considering the radiation zone, where $|\bar{r} - \bar{r}'| >> |\bar{r}'|$ or $r >> r'$ the lowest order potential terms contribute to radiated fields as

$$\bar{E}^e(r) = -j\omega\bar{A} \tag{13}$$

$$\bar{H}^e(r) = \left[\frac{1}{\eta_o}\right] \hat{n} \times \bar{E} = \left[\frac{-j\omega}{\eta_o}\right] \hat{n} \times \bar{A} \tag{14}$$

and

$$\bar{H}^m(r) = -j\omega\bar{F} \tag{15}$$

$$\bar{E}^m(r) = \left[\frac{1}{\eta_o}\right] \bar{H} \times \hat{n} = \left[\frac{-j\omega}{\eta_o}\right] \bar{F} \times \hat{n} \tag{16}$$

where the free space impedance $\eta_o = 120\pi\ \Omega$.

Using the far field approximation, the radiation fields due to equivalent sources $\bar{K}$ and $\bar{M}$ are

$$\bar{E}(r) = \left[\frac{-j\omega\mu}{4\pi}\right] \frac{e^{-jk_o r}}{r} \iint_s \bar{K}(\bar{r}')\, e^{-jk_o r' \cos\varphi}\, ds' \tag{17}$$

$$\bar{H}(r) = \left[\frac{-j\omega\varepsilon}{4\pi}\right] \frac{e^{-jk_o r}}{r} \iint_s \bar{M}(\bar{r}')\, e^{-jk_o r' \cos\varphi}\, ds' \tag{18}$$

where φ is the angle between position vectors $\bar{r}$ and $\bar{r}'$.

The major problem in microstrip antenna analysis is the determination of the equivalent current distributions $\bar{K}$ and $\bar{M}$ for the specified geometry. The popular approach is to follow the integral equation formulation and use the method of moments to generate numerical results due to such current distributions. Formulation of the integral equation for the unknown currents on the patch and feed line can be carried out with the help of the enforcement of the boundary

conditions on the conducting surfaces. The vanishing tangential component of the total electric field requires

$$\hat{n} \times \bar{E}_{tot} = 0 \tag{19}$$

on the conducting surfaces, $\bar{E}_{tot}$ can be obtained with the help of equation (9). The radiated power is obtained by integrating the Poynting vector along the equivalent aperture .

$$P_r = \left[\frac{1}{2}\right] \mathrm{Re} \iint_{aperture} (\bar{E} \times \bar{H}^*) \cdot \bar{ds} \tag{20}$$

The dissipated power consists of conductor and dielectric losses. Conductor losses are given by

$$P_c = R_s \iint_S (\bar{K} \cdot \bar{K}^*)\, ds \tag{21}$$

where R_s is the real part of the surface impedance, S is the patch area and dielectric losses are given by

$$P_d = \left[\frac{\omega \varepsilon''}{2}\right] \iiint_V |E|^2 \, dv \tag{22}$$

where ε'' is the imaginary part of the permitivity, if dielectric losses are taken into account, then it is assumed that $\varepsilon = \varepsilon' + j\varepsilon''$.

Readily available computer packages that employ Method of Moments to solve integral equations are used extensively to determine performance of microstrip antennas. However, the output variables we have access to, are only limited to scattering parameters at the user

defined ports. Information provided by scattering parameters leads to accurate determination of bandwidth characteristics and quantifies approximately the radiation efficiency of the overall structure. Unfortunately, since no provisions were made in these packages, we could not determine the radiation patterns associated with the structures investigated in this work.

CHAPTER III

NUMERICAL SIMULATIONS

The wideband microstrip antenna addressed in this thesis requires complex analytical formulation and extensive numerical evaluations. Proposed solution involves a multi-layered structure which makes the solution even more difficult. Though the available computer packages for electromagnetic analysis of microstrip structures are limited in their performance, it is still practical to utilize them if they achieve reasonable accuracy.

Electromagnetic Microwave Design Software (EM)

The accuracy in analyzing planar microstrip patches in layered dielectric structures depends on how discontinuities are treated. This accuracy can further be improved by proper consideration of losses (metalization, dielectric and radiation) and by including the feed structure. Furthermore, accuracy can be enhanced by optimizing the step size involved in numerical evaluations. The EM (Electromagnetic Microwave design software) package by Sonnet Software, meets most of these requirements. However, it is still restricted in its output variables, being limited only to scattering parameters at user defined ports. Since there is no access to the source code, it is not possible to make use of the evaluated current distributions to predict radiation patterns. However, the information obtained from the scattering parameters enables us to determine the bandwidth characteristics and also yields some estimates for the radiated power.

Xgeom is an X Window, mouse based program that captures microstrip circuit geometry which is used as an input to the Electromagnetic Microwave design package (EM). Xgeom can capture any number of arbitrary patch geometries located in a multilayer dielectric medium of finite extent. Each dielectric layer can be characterized in terms of physical thickness, relative dielectric constant and loss tangent. The planar geometry is subdivided into subsections and there is no limit to the number of subsections that can be chosen. The larger the number of subsections, the longer is the analysis time. To activate Xgeom, the command " Xgeom Example.geo & " and pressing return is sufficient. While Xgeom is running the Xgeom window displays a square outline of the default substrate with a grid indicating default subsections. A menu of options is displayed in the upper part of the window to enable the user to switch in between modes and to insert circuit specifications via control of the mouse. By choosing sequential options, the box parameters (area, cell size, circuit symmetry and number of levels), the substrate parameters (thickness, dielectric constant and loss tangent) and all remaining patch parameters (geometry, ports, reference planes, vias, etc.,) can be specified. The generated input file describing the geometry is ready to be analyzed by EM. A menu summary is shown in Figure 6 and a sample circuit as seen on the screen is shown in Figure 7 [10].

EM is a practical electromagnetic analysis program which evaluates S-parameters for arbitrary microstrip geometries with high accuracy. It performs an electromagnetic analysis of microstrip circuits by solving

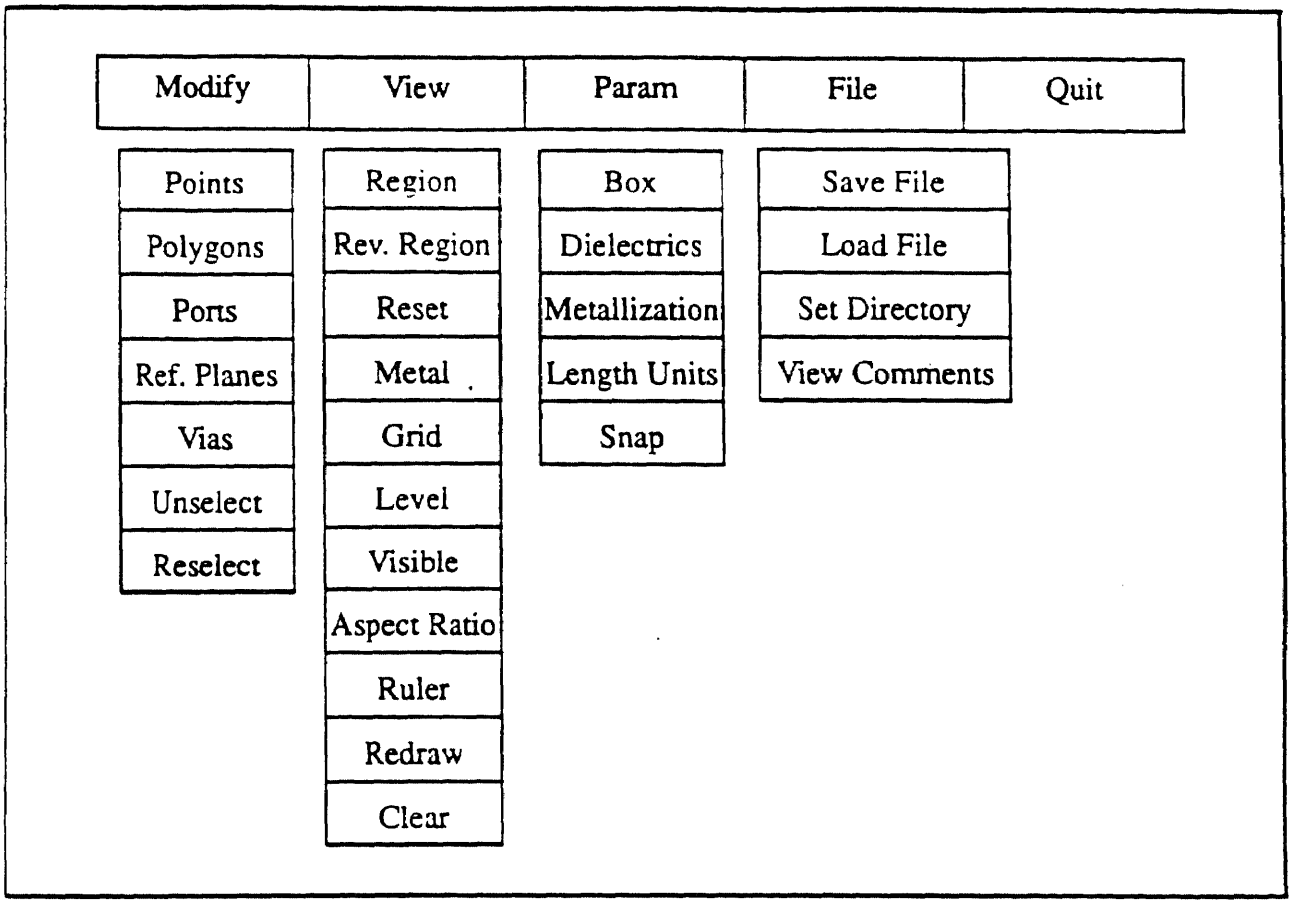

Figure 6. Menu summary of the Xgeom package.

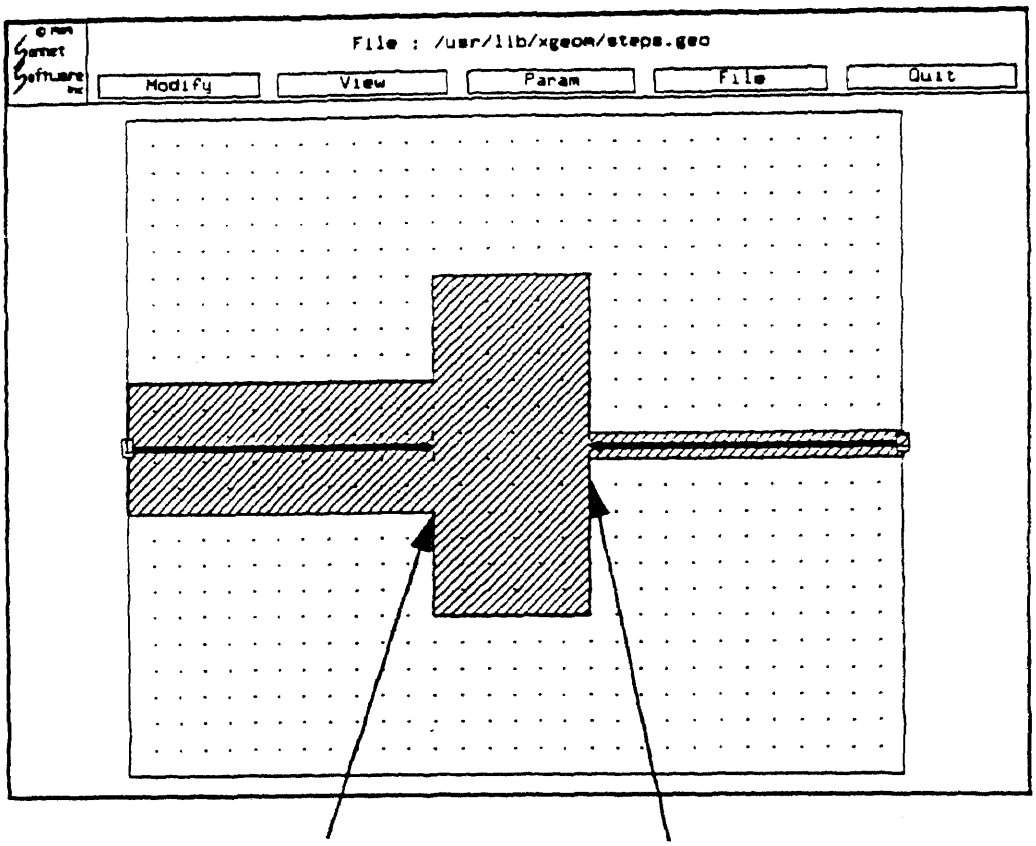

Figure 7. A sample circuit representation on the screen

for the current distribution in the microstrip metallization. Basically it solves the integral equation (17) using the method of moments. EM analyzes given structures inside a shielded box where port connections are made at the box side walls (Figure 8). The analysis inherently includes dispersion, metallization losses, dielectric losses and radiation losses [9]. Theoretically it can handle any number of ports, any number of layers, any number of subsections, any number of frequencies in any frequency range. However, it is limited with the speed and the memory of the platform on which it is executed. The platform used in this thesis is Apollo DN4500 Workstation. The first step of the solution involves evaluation of the tangential electric field on all cells (subsections). Each cell contributes to the electric field in remaining cells. Collective contribution due to all cells yields the final field. But since the total tangential electric field must be zero on the surface of any conductor, EM assumes currents on all cells simultaneously and adjusts these currents such that the total tangential electric field vanishes on the conducting surface. The numerically determined currents along individual cells collectively represent current distributions induced on metallic patterns. The S-parameters are determined using these current distributions. When metallization loss is available, boundary conditions are modified and the analysis is carried out accordingly [3]. The sample input and output files for a specific example are given in Appendix A.

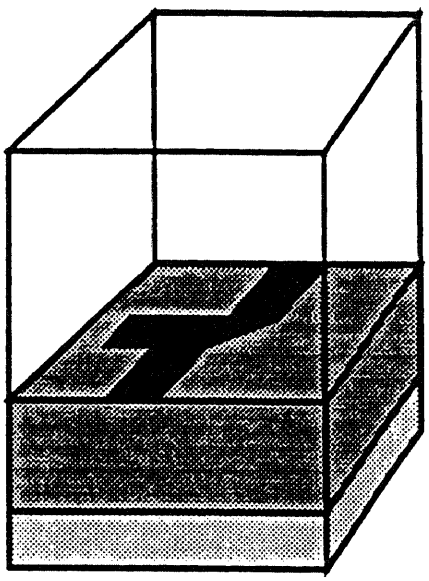

Figure 8. Box enclosure used for analysis by EM software package

Chapter IV

VALIDATION OF NUMERICAL EVALUATIONS

Validating the computed results is essential to developing confidence in any proposed model. Generally, computer codes are developed to address problems which could not be solved analytically. Code developers tend to consider that validation is accomplished when some of the more generic analytically solvable cases tend to agree with the produced numerical results. Users of these codes, on the other hand, more often will be attempting solutions of problems for which analytical solutions are unavailable and experimental data may itself be an unreliable validation source [5]. Hence, validation will be a continuing requirement, especially as larger and more complex problems are attempted and as new codes are introduced.

The validity and accuracy of numerical results generated by EM code was determined by comparing them with numerical data obtained by other codes and experimental results published in the open literature. The geometry chosen for such a validation includes a rectangular patch antenna placed on a dielectric substrate over a ground plane as shown in Figure 9.The patch is connected via the feed line into an external port. The scattering parameter S_{11} corresponds to a reflection coefficient which indicates the performance of this structure as a possible cavity. The minimum value of the magnitude of the reflection coefficient occurs at a frequency which corresponds to a resonance frequency of an equivalent cavity. If internal losses are neglected, this approximately corresponds to the frequency at which maximum power

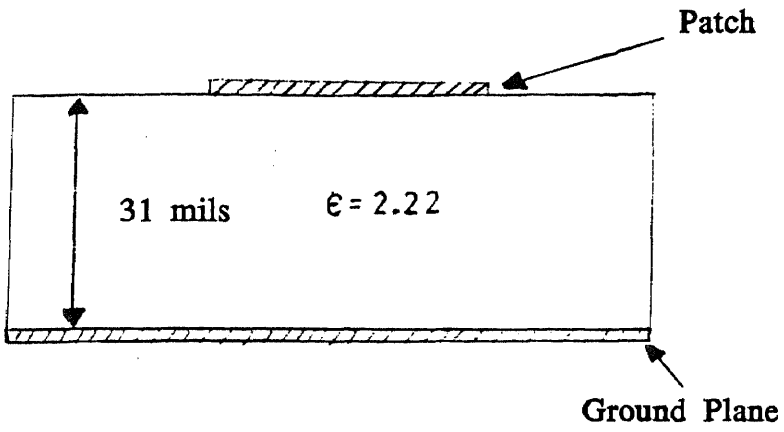

a) Crossectional view

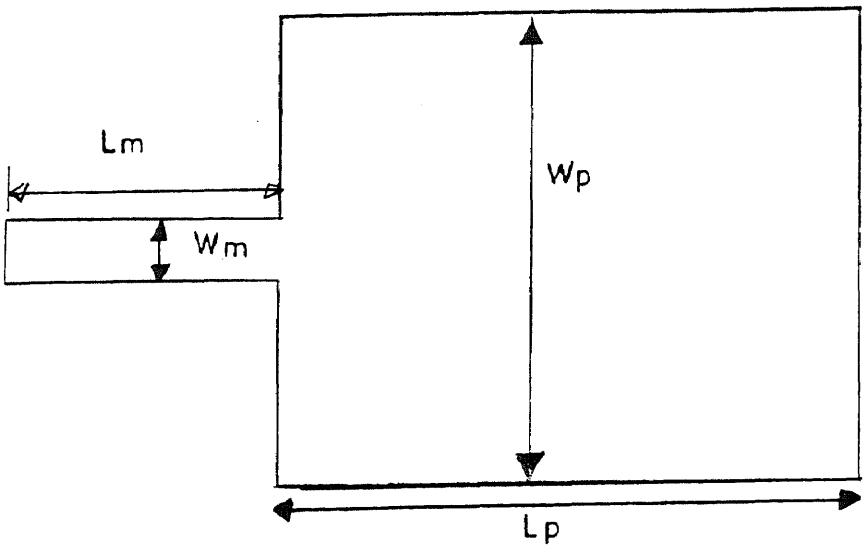

b) Patch geometry

Figure 9. End-fed rectangular patch antenna.

is radiated from this structure. Figure 10 depicts the variation of $|S_{11}|$ versus frequency. The minimum value of $|S_{11}|$ is approximately determined at a frequency of 8.9 GHz. Further, expanded results around the resonance are presented in Figure 11, where the resonance frequency of 8.92 GHz is now determined more accurately. The physical parameters associated with the patch are W_m=90, L_m=200, W_p=538.50 and L_p=432.35 mils.

Comparison of numerical results generated by EM package with available data is given in Table 1. EM results are compared with ones reported previously [9] included data generated by Touchstone package (TA), Transmission Line Model (TLM), the Cavity Model (CM) and experimental measurements. They all are included in Table 1. The percentage error obtained for all numerical methods based on experimental data is also listed in Table 1. Comparison are carried out for various patch dimensions and the percentage error remained less than 8.0%. Numerical results generated by EM package show that there is substantial agreement with other methods and experimental data. It gives enough confidence to use EM package for further investigations in microstrip antenna analysis.

Figure 10 Reflection Coefficient versus frequency for the microstrip antenna in (Figure 9). (Wp=538.50,Lp=432.35)

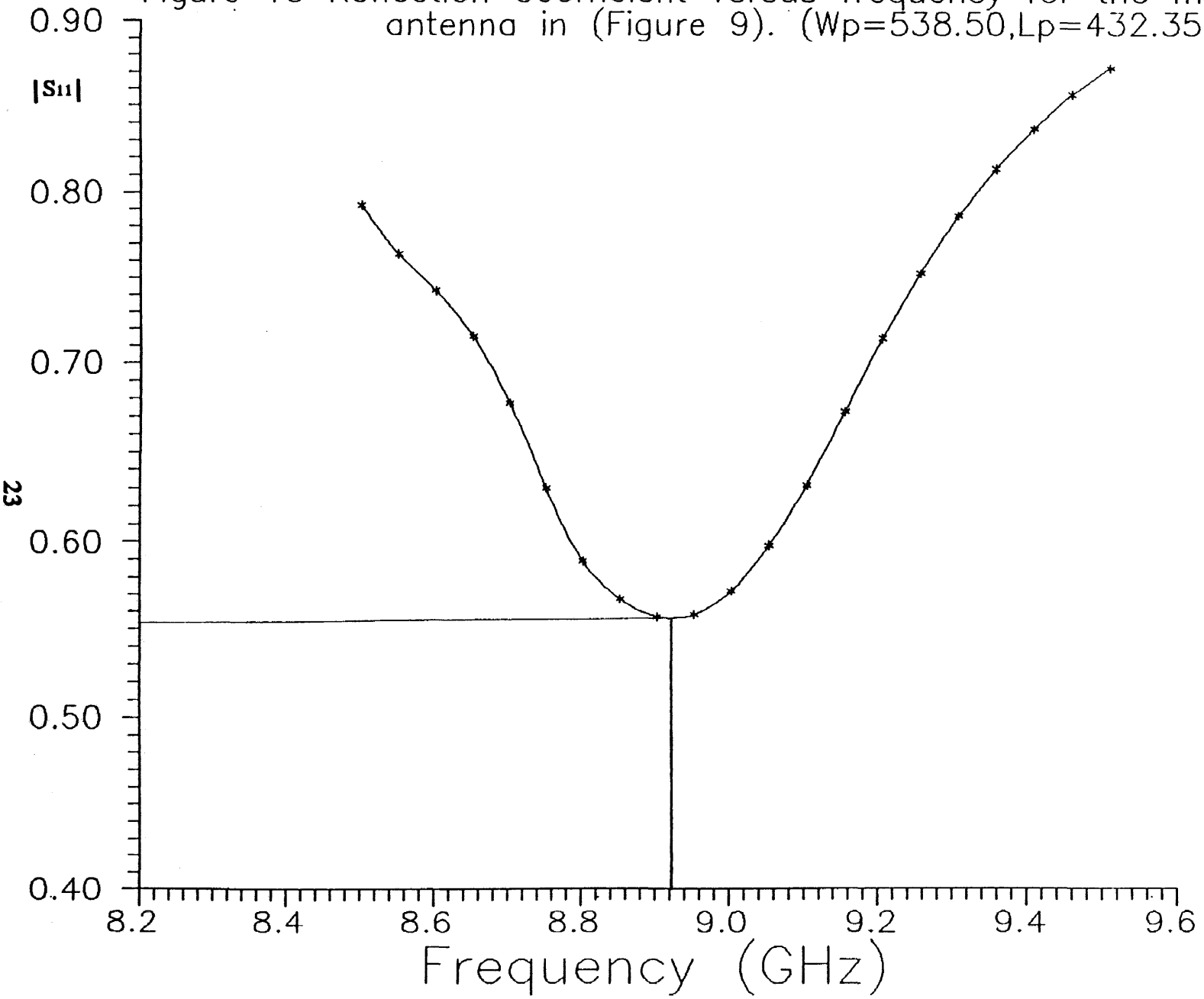

Figure 11 More accurate representation of the reflection coefficient around the resonance frequency

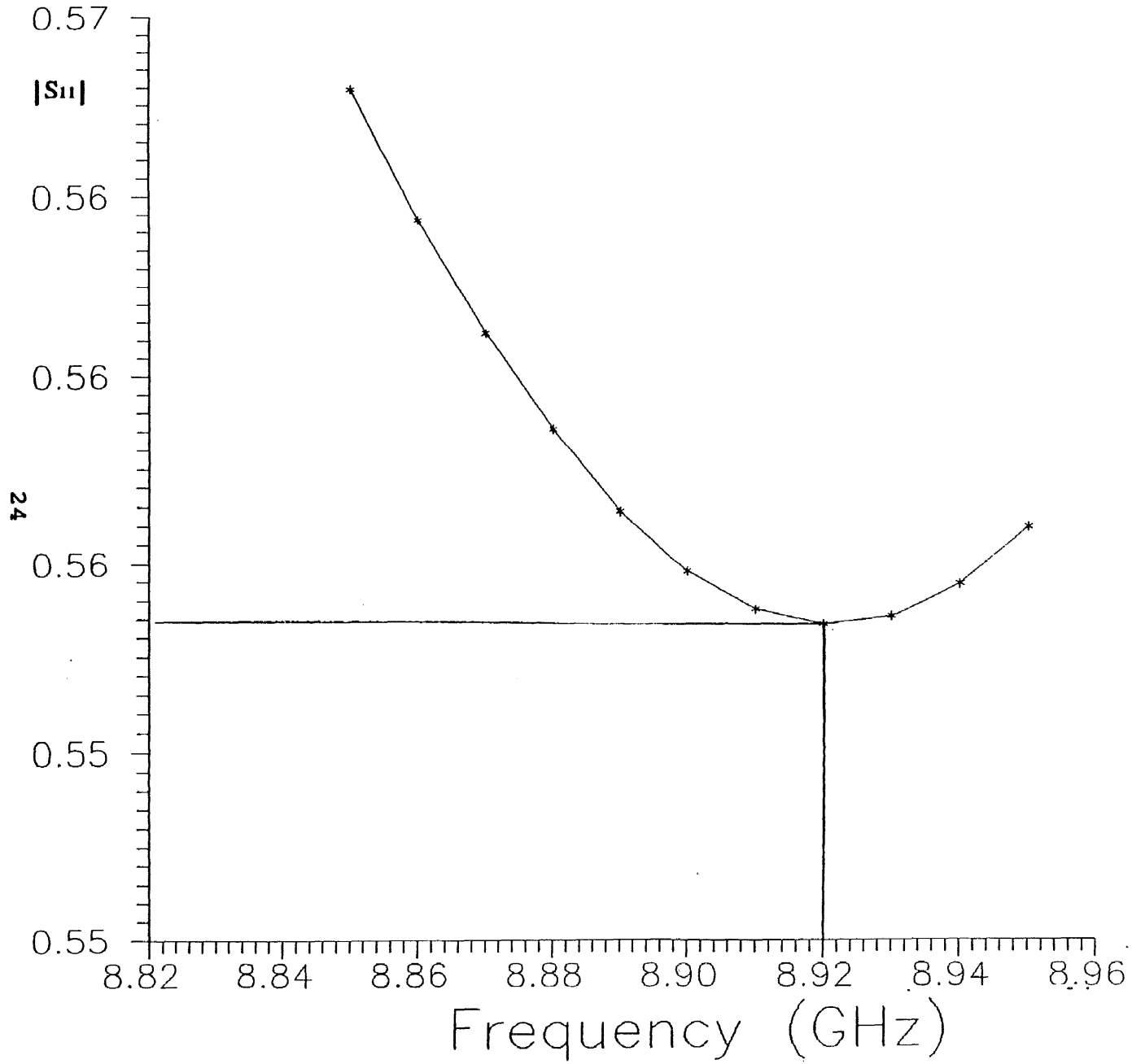

Patch Width [mils]	Patch length [mils]	Resonant Frequency (GHz) Em	TA	TLM	CM	Expt	Percentage Error % Em	TA	TLM	CM
537.80	410.65	9.17	8.79	9.08	8.88	8.74	-4.95	-0.60	-3.93	-1.61
538.50	432.35	8.92	8.40	8.66	8.49	8.48	-5.19	0.94	-2.08	-0.07
536.85	472.30	8.06	7.76	7.97	7.84	7.96	-1.26	2.51	-0.14	1.46
539.30	452.40	8.81	8.07	8.30	8.15	8.30	-6.14	2.77	0.02	1.80
480.55	452.40	8.50	8.60	8.84	8.76	8.73	2.58	1.43	-1.34	-0.36
482.65	403.60	9.39	8.96	9.24	9.07	9.23	-1.73	2.93	-0.11	1.74
481.70	383.35	10.18	9.38	9.69	9.49	9.46	-7.61	0.85	-2.44	0.27
481.60	363.65	10.35	9.82	10.2	9.93	9.64	-7.36	-1.87	-5.53	-2.96

Table 1. Comparison of computed and experimental data
(h = 31 mil , ε = 2.22 , Wm = 90 mil , Lm = 200 mil)

CHAPTER V

NUMERICAL RESULTS

The performance of a microstrip antenna is dependent on its physical parameters. One of the primary goals of this thesis is to obtain wide band performance, which can be determined using EM package.

Bandwidth Optimization of a Microstrip Dipole

It is a well known fact that microstrip antennas have very narrow bandwidths. This is mainly due to their operation as resonance cavities. However, substrate parameters (thickness and dielectric constant) can be optimized to get the best possible bandwidth out of the specified geometry. This has been well documented in the literature [1]. Numerical results presented in Figure 12 show quite complicated bandwidth response of the dipole microstrip antenna. The theoretical definition of the bandwidth defined in Figure 12 is given as [1]

$$BW = \frac{1}{L_r} \frac{2\ R_r}{\frac{dX_{in}}{dL_\lambda}\Big|_L} \tag{23}$$

where L_r is the resonance length, R_r is the resonance resistance, $L_\lambda = \frac{L}{\lambda}$ is the normalized length and X_{in} is the input reactance.

Curves in Figure 12 suggest that bandwidth can be optimized for various values of substrate thickness provided that all other remaining parameters are kept constant. Physically it corresponds to excitation of more modes as the thickness of the substrate is increased. The

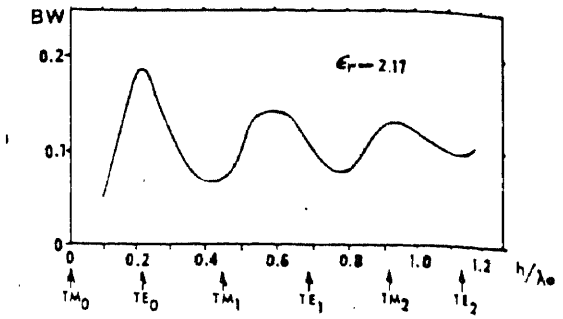

a) $\varepsilon=2.17$

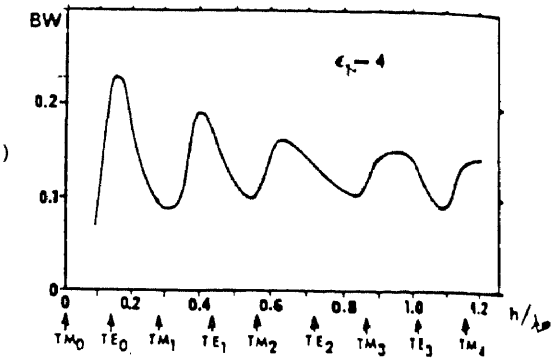

b) $\varepsilon=4$

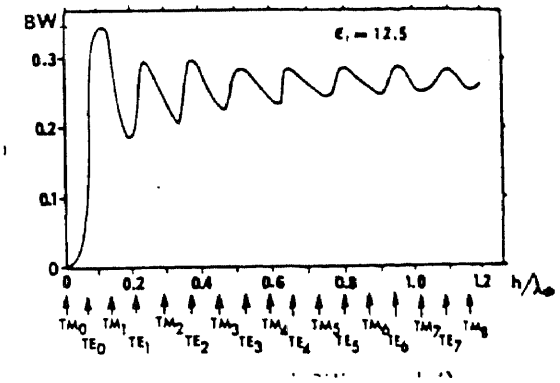

c) $\varepsilon=12.5$

Figure 12. Bandwidth performance of the dipole microstrip antenna versus substrate thickness.

oscillations in these curves are primarily due to collective interference of these exited modes. For the optimized parameters, the bandwidth performance is maximum. As the critical parameter is deviated from the optimum value, the bandwidth starts to decrease.

This optimization scheme has been extended to study bandwidth performance of rectangular microstrip patch antenna (Figure 13) in this thesis. Theoretical definition in (23) is no longer used because the parameters involved are not readily available. Hence, an approximate way to estimate the bandwidth is preferred, which is based on the choice of tolerable maximum value of the reflection coefficient magnitude, $|S_{11}|_{max}$. If this choice corresponds to $|S_{11}|_{max}$= 0.6, then the radiated power (incident - reflected) is approximated as (assuming no losses inside the structure).

$$P_{rad} \tilde{=} P_{inc}(1-|\rho|^2) \geq P_{inc}(1-|S_{11}|^2_{max})=0.64\ P_{inc} \qquad (24)$$

Though there are various approximations involved in the above expression, it gives a good estimate for radiated power in the determined bandwidth.

Figures 14-24 show variation of $|S_{11}|$ versus frequency in the increasing thickness of the substrate. The thickness varies from 62 mils to 400 mils. The bandwidth is approximated according to the maximum tolerable reflection coefficient magnitude $|S_{11}|_{max}$=0.6. The curves in Figures 14-24 exhibit oscillatory patterns which are a consequence of interference of additional modes introduced as the thickness is increased. The bandwidth variation determined from Figures 14-24 is outlined in Table 2. Figure 25 exhibits bandwidth

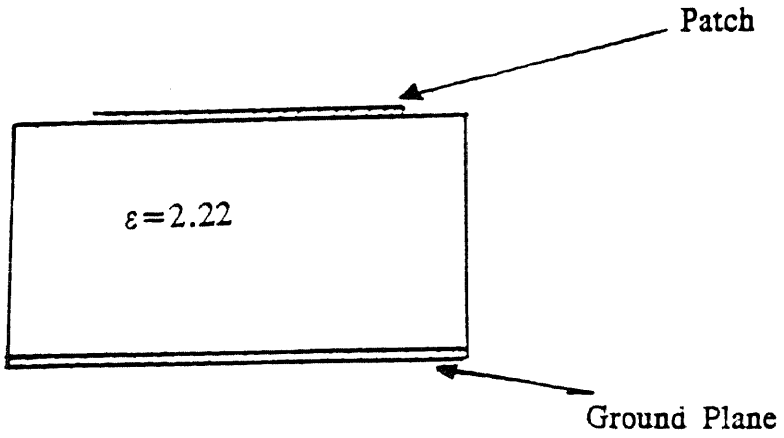

a) Crossectional view

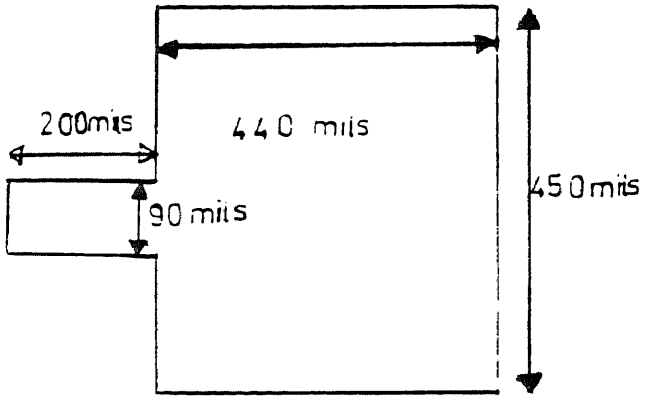

b) Patch geometry

Figure 13. Rectangular patch antenna.

Figure 14 Bandwidth performance versus frequency for substrate thickness of 62 mils. BW = 1.07 GHz

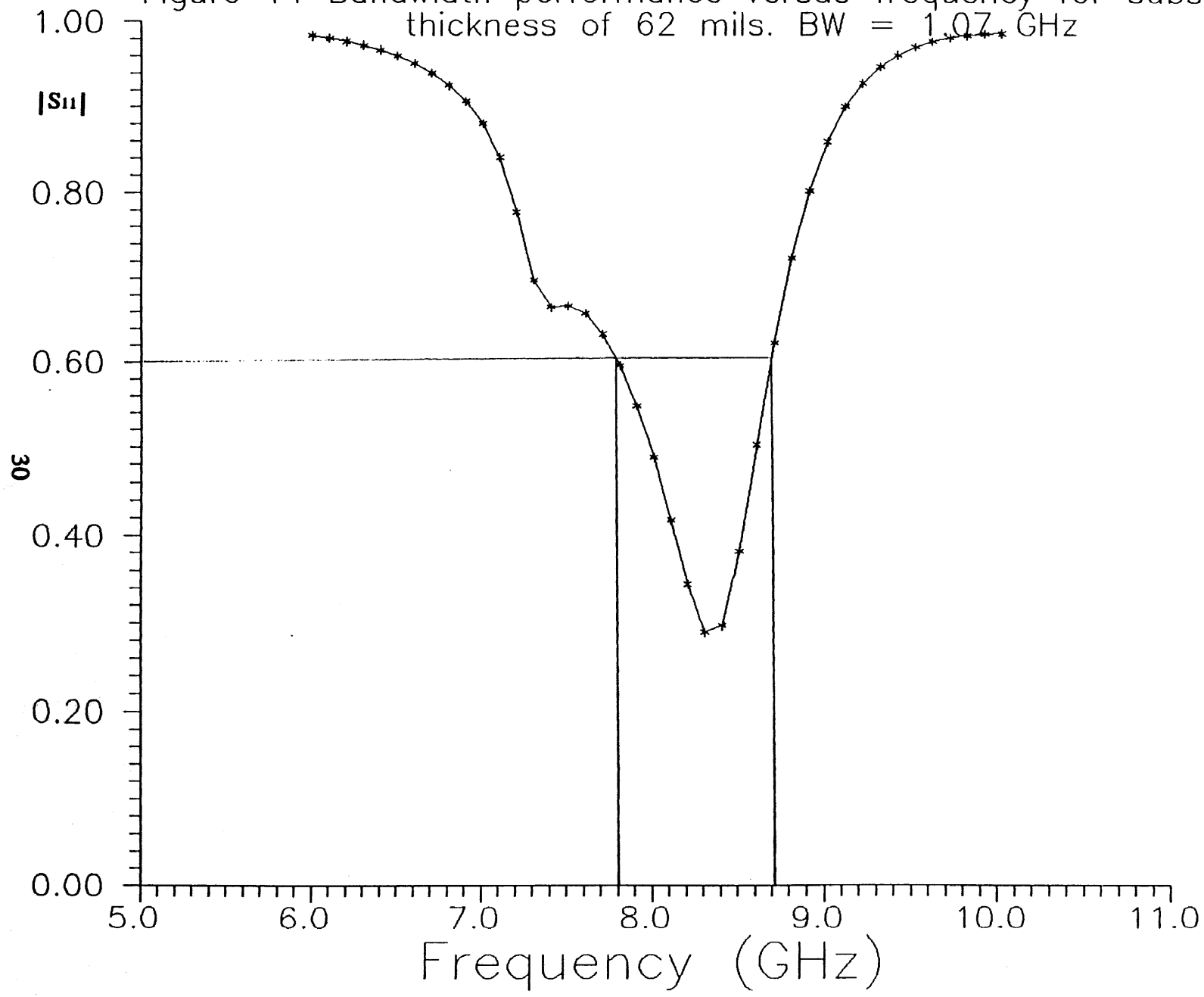

Figure 15 Bandwidth performance versus frequency for the substrate thickness of 90 mils. BW = 1.35 GHz.

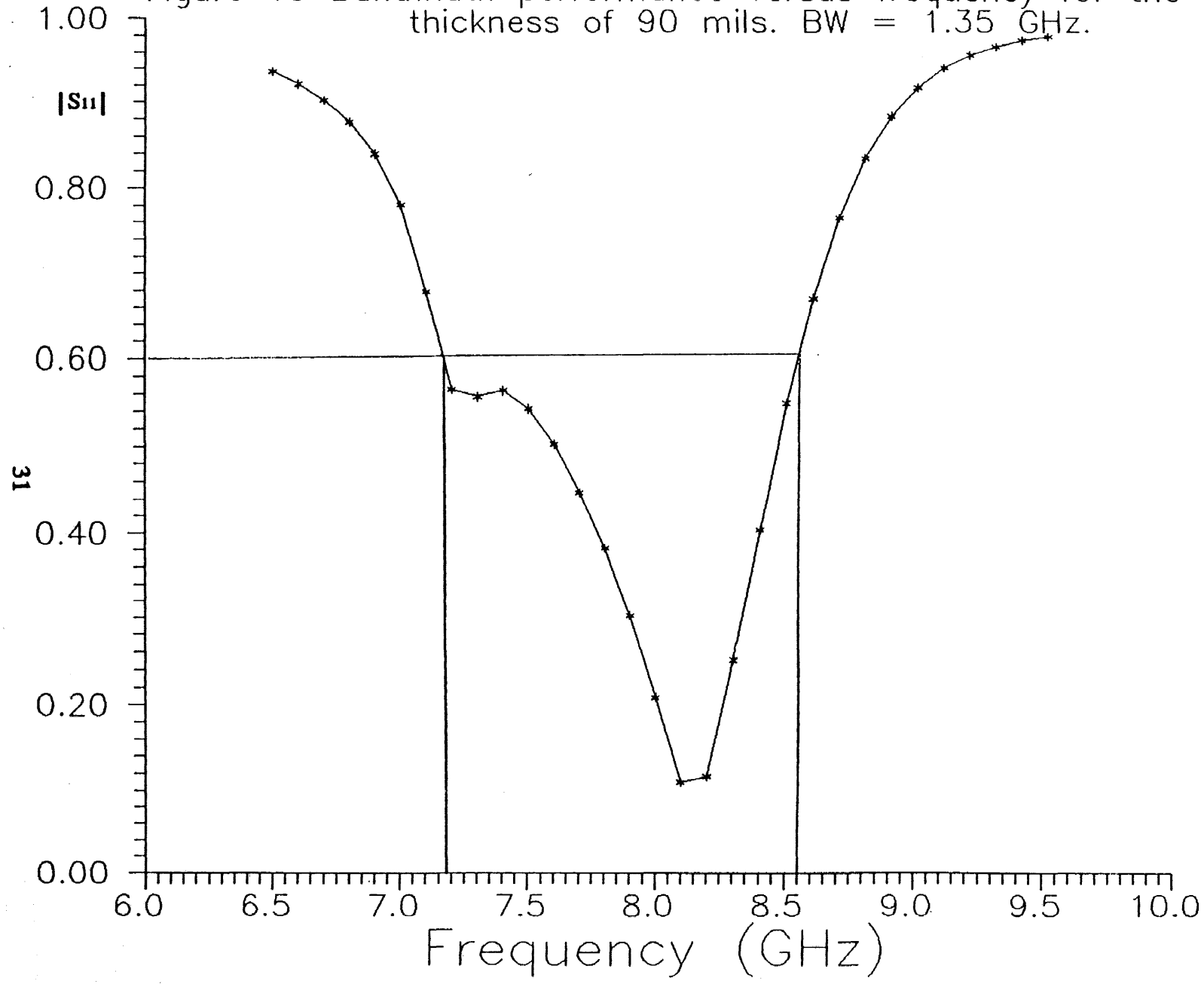

Figure 16 Bandwidth performance versus frequency for the substrate thickness of 120 mils. BW = 1.45 GHz.

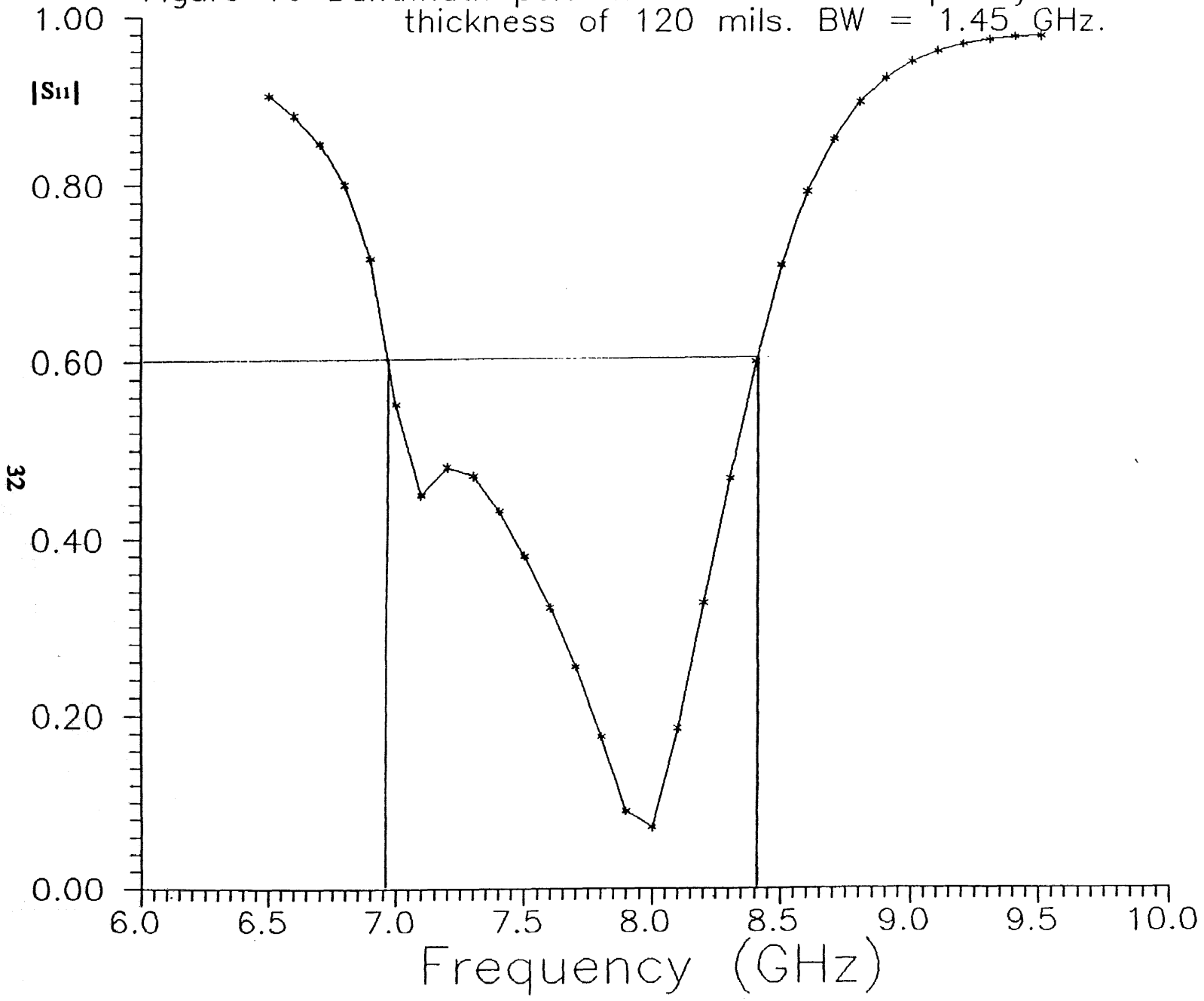

Figure 17 Bandwidth performance versus frequency for the substrate thickness of 150 mils. BW = 1.47 GHz.

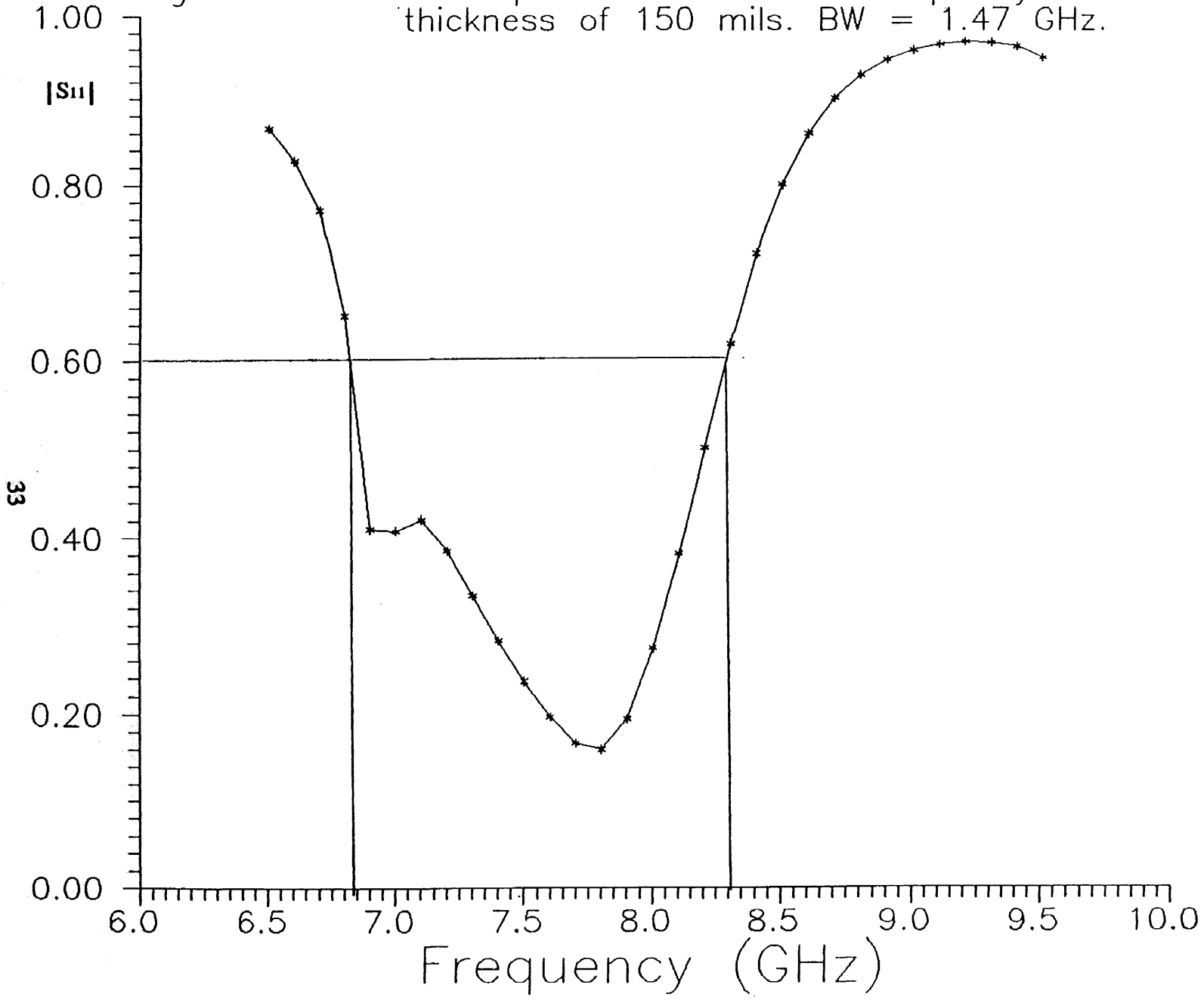

Figure 18 Bandwidth performance versus frequency for the substrate thickness of 165 mils. BW = 1.50 GHz.

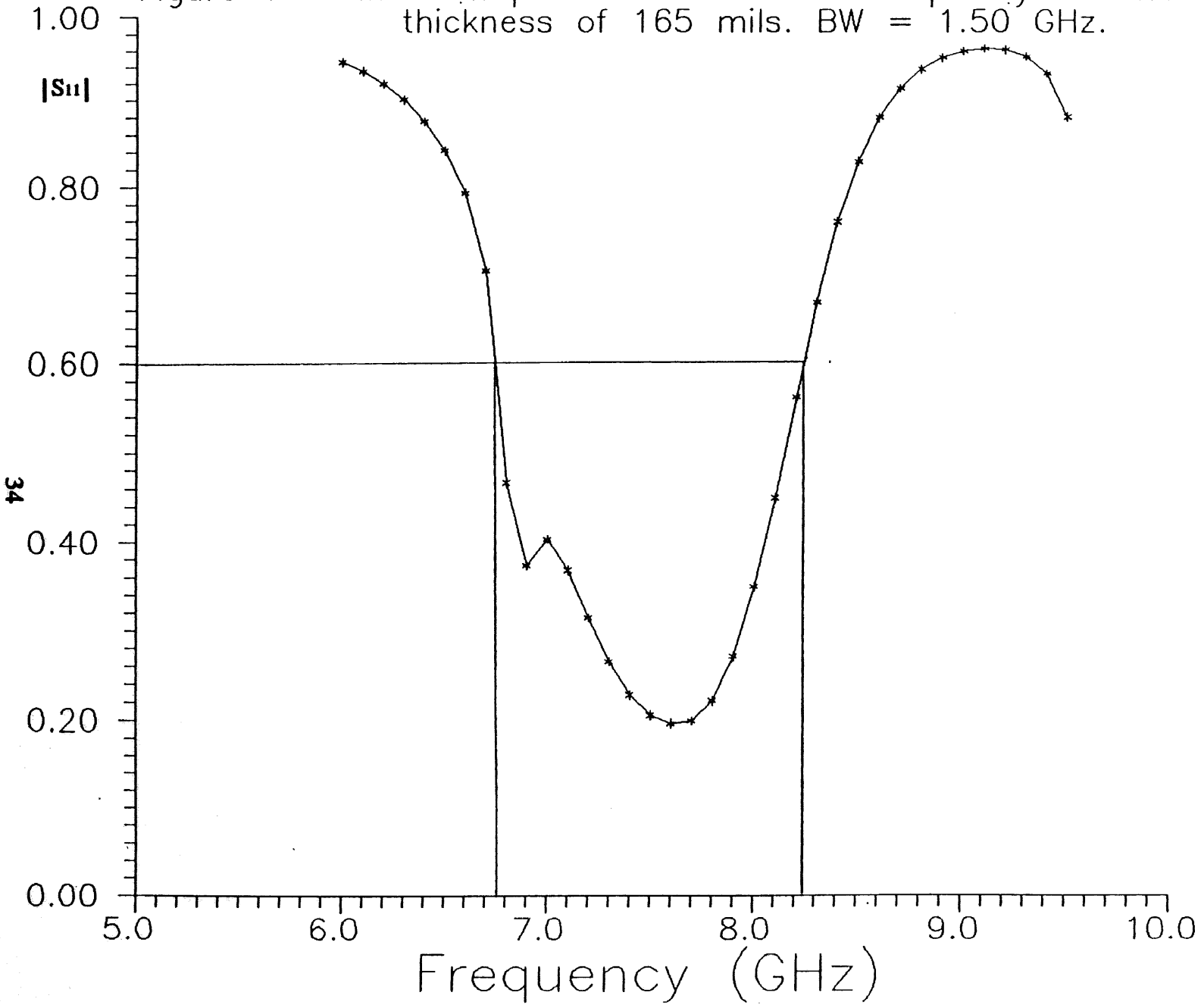

Figure 19 Bandwidth performance versus frequency for the substrate thickness of 180 mils. BW = 1.53 GHz.

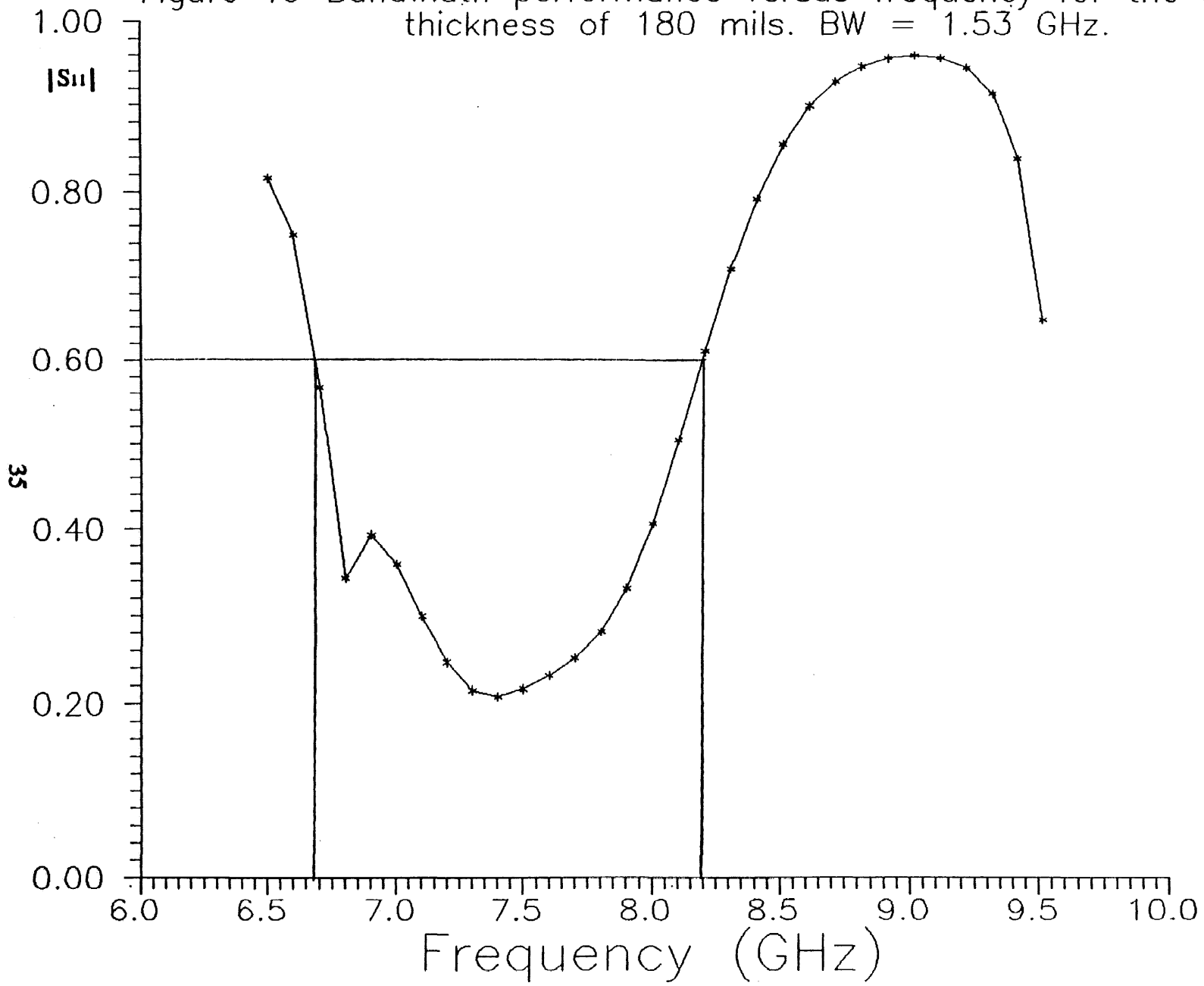

Figure 20 Bandwidth performance versus frequency for the substrate thickness of 200 mils. BW = 1.56 GHz.

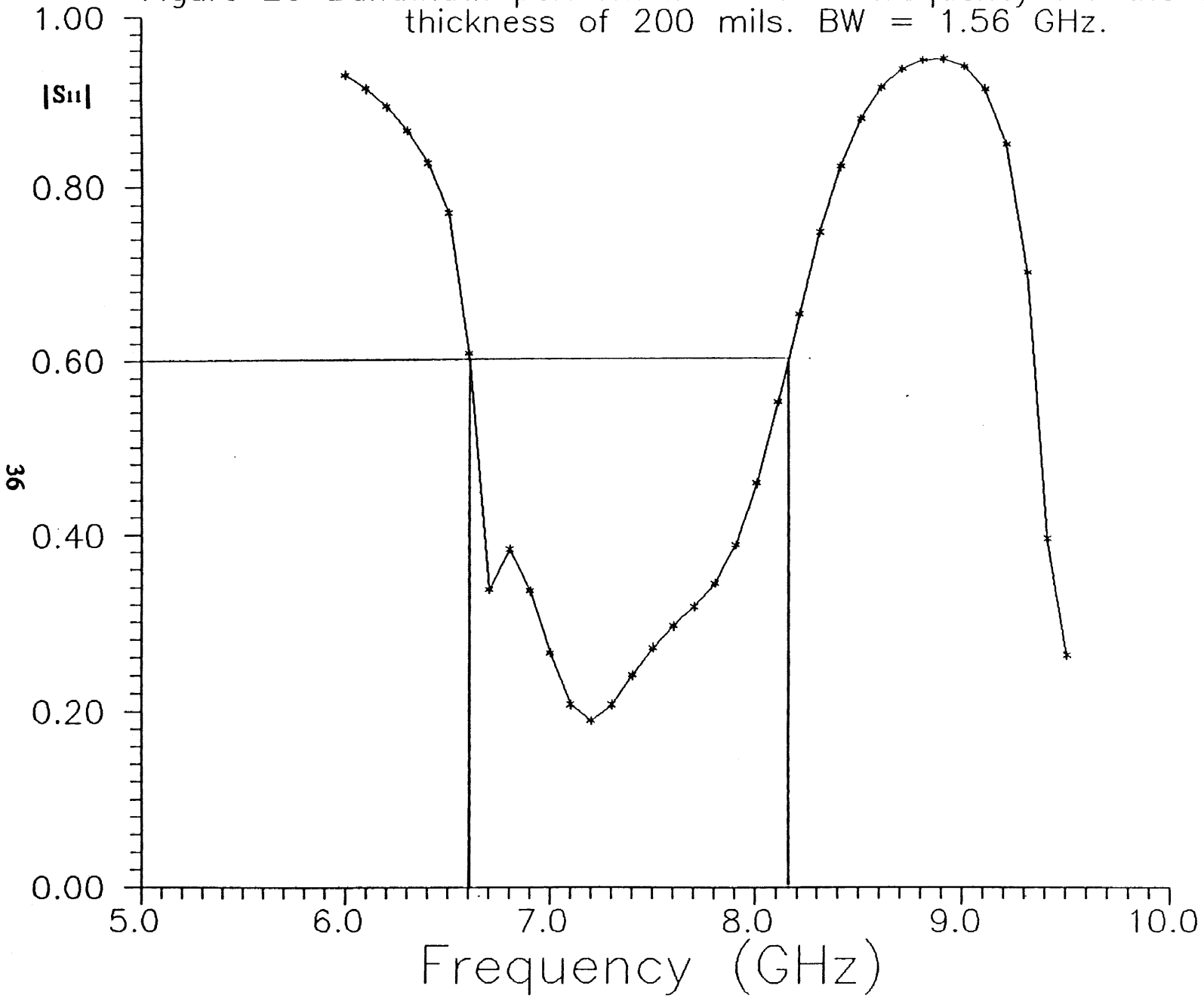

Figure 21 Bandwidth performance versus frequency for the substrate thickness of 220 mils. BW = 1.62 GHz.

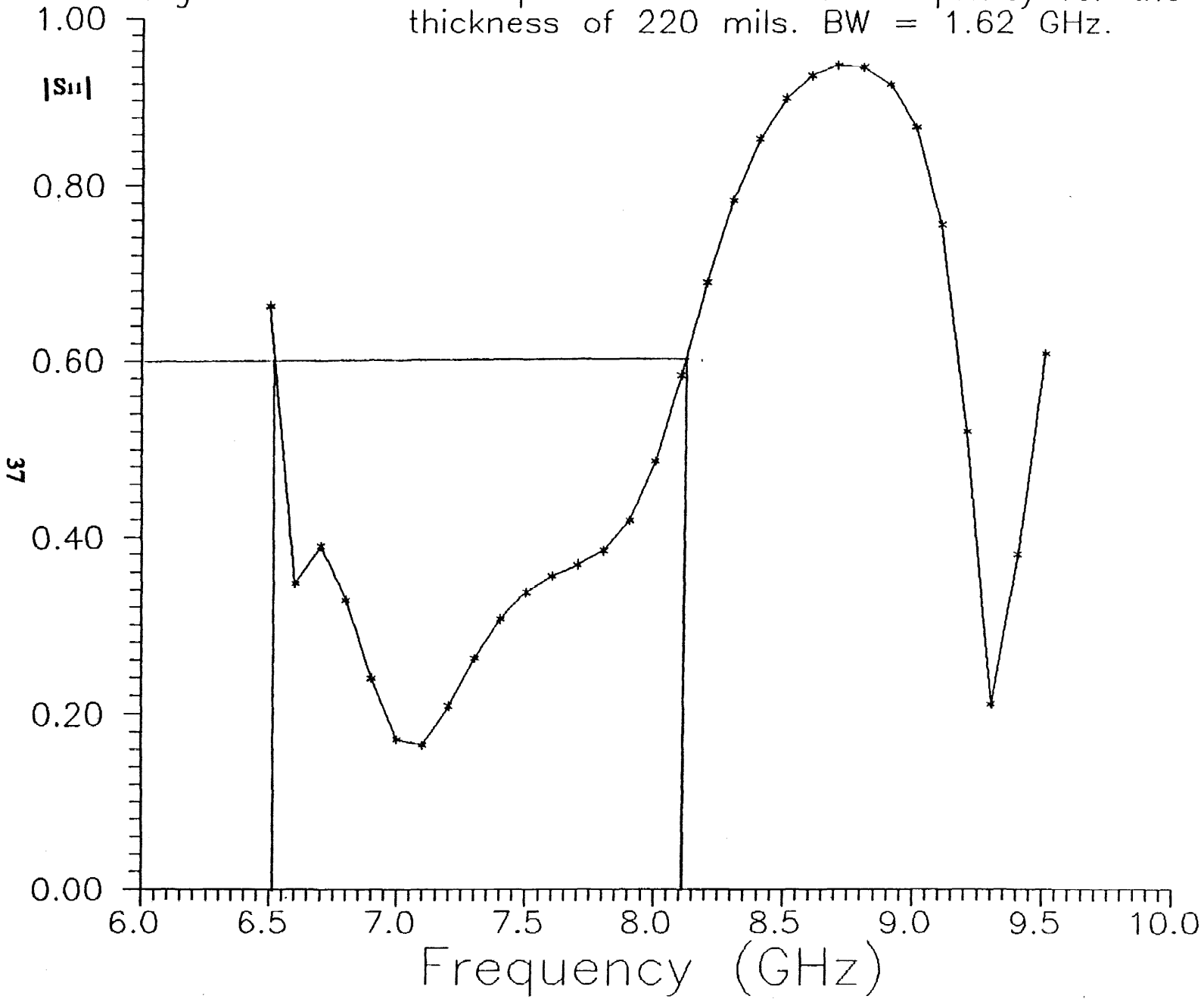

Figure 22 Bandwidth performance versus frequency for the substrate thickness of 260 mils. BW = 1.75 GHz.

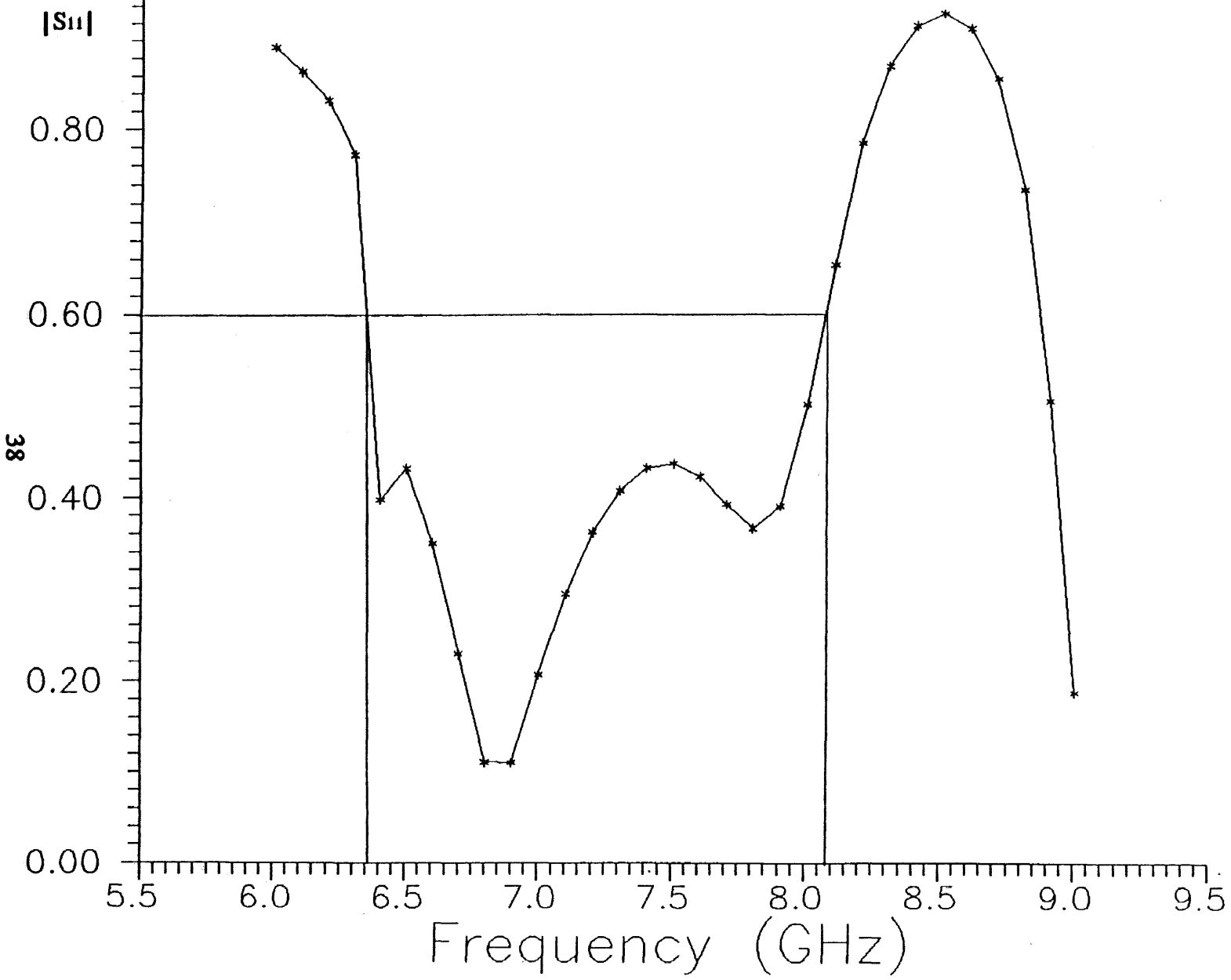

Figure 23 Bandwidth performance versus frequency for the substrate thickness of 320 mils. BW = 1.67 GHz.

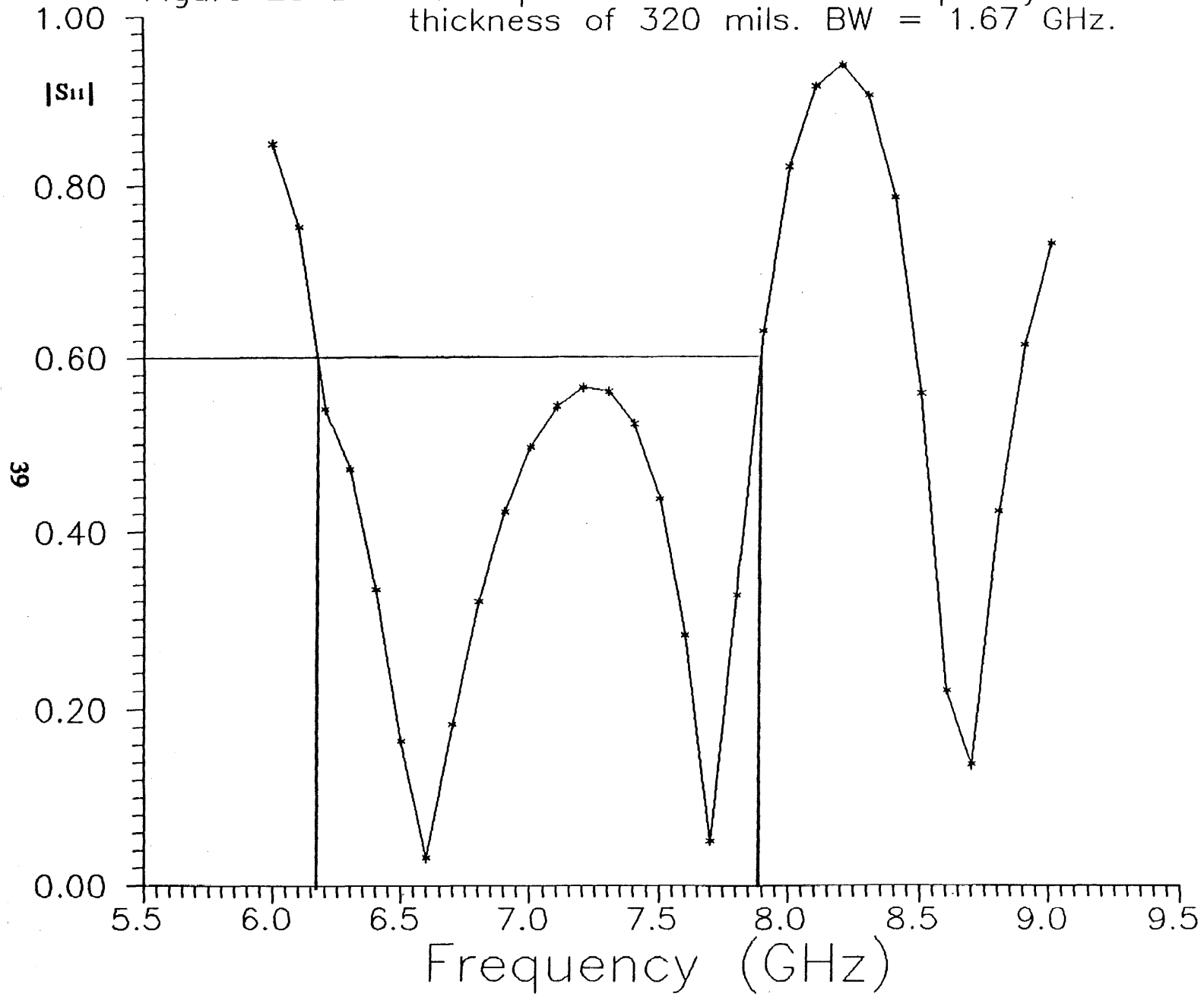

Figure 24 Bandwidth performance versus frequency for the substrate thickness of 400 mils. BW = 0.65 GHz.

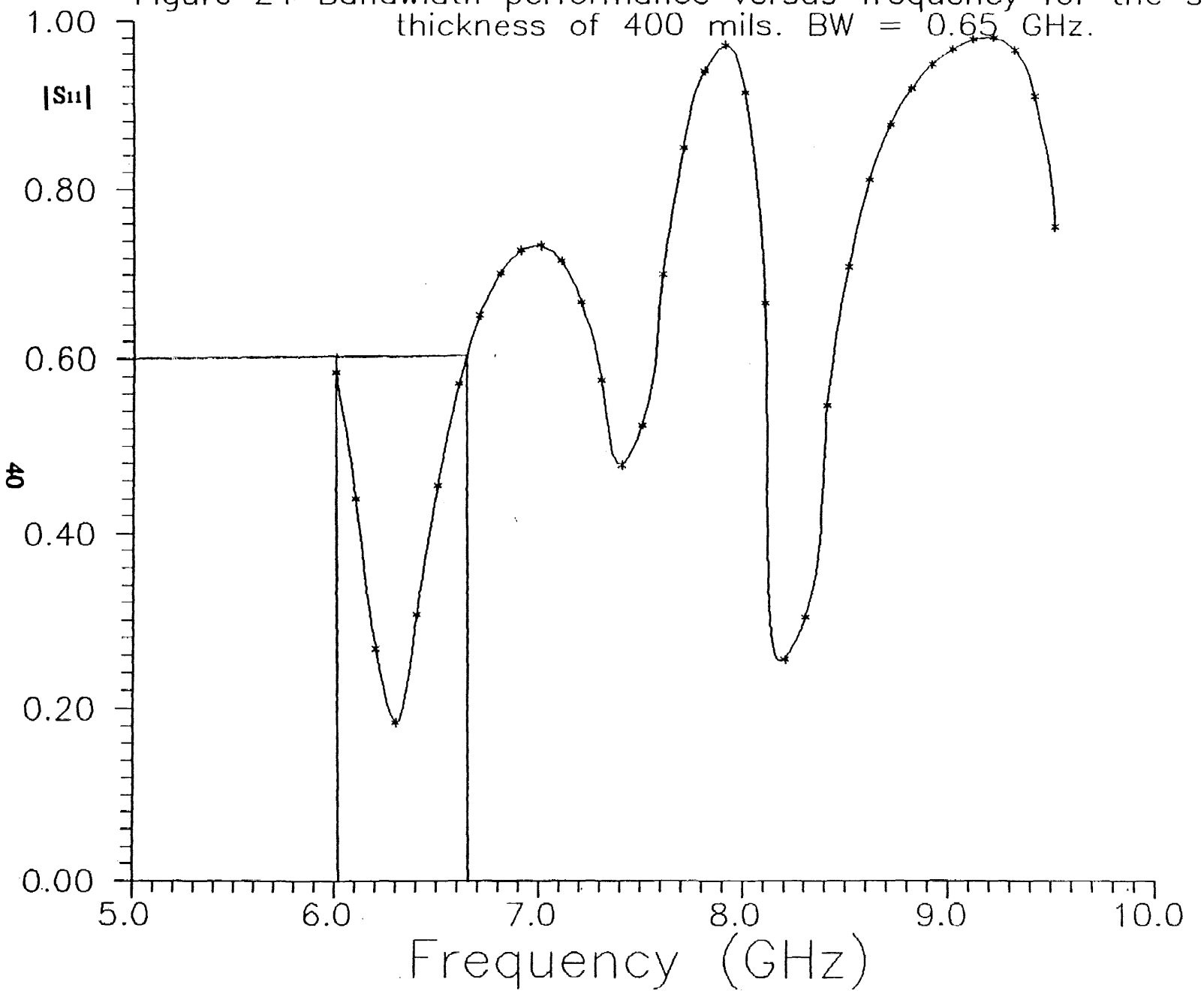

Thickness [mils]	Resonance frequency [GHz]	Bandwidth [GHz]	h/λo	Plot Fig No
62	8.3	1.07	0.0436	14
90	8.1	1.35	0.0617	15
120	8.0	1.45	0.0813	16
150	7.8	1.47	0.0991	17
165	7.6	1.50	0.1062	18
180	7.4	1.53	0.1128	19
200	7.2	1.56	0.1219	20
220	7.1	1.62	0.1323	21
260	6.9	1.75	0.1519	22
320	6.6	1.67	0.1788	23
400	6.3	0.65	0.2134	24

Table 2. Bandwidth optimization of the rectangular patch antenna versus substrate thickness.

Figure 25 Bandwidth performancce versus substrate thickness normalized with free space wavelength

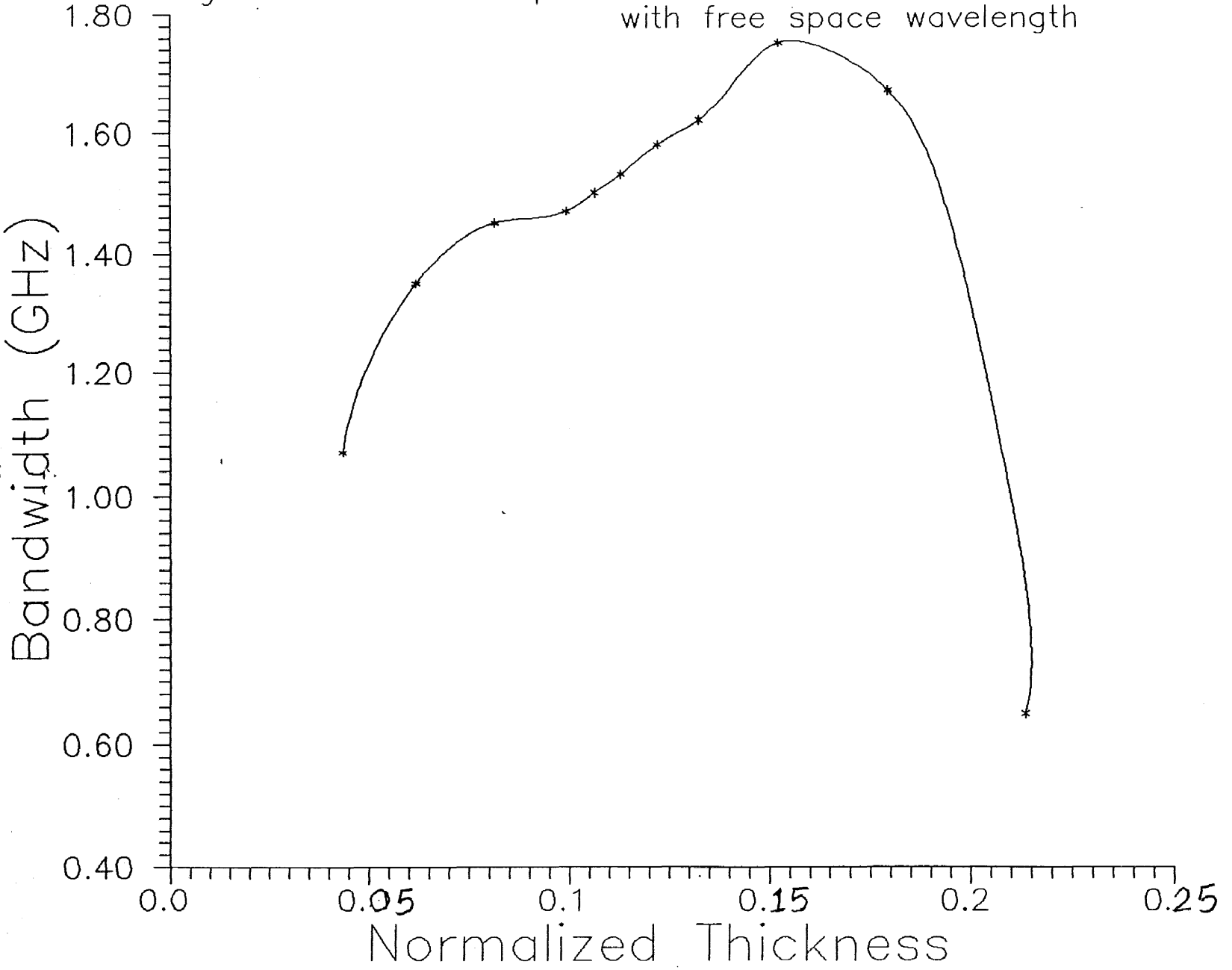

variation versus substrate thickness yielding the optimum performance at BW = 1.75 Ghz for substrate thickness of 260 mils. Any deviation from this optimum thickness results in a decrease of the available bandwidth.

Bandwidth Optimization of a Rectangular Patch at Radio Frequencies

The goal of this thesis is to optimize a microstrip antenna in the frequency band covering 400-500 Mhz. The extension of the optimization in the previous section is also applicable here. However, the physical dimensions of the antenna should be such that it will fit into an average size briefcase (45cm × 55cm × 13cm). The rectangular patch investigated in this section is shown in Figure 26. Numerical optimization for this antenna is carried out in two steps. Initially, the optimization parameter is chosen to be the substrate thickness. Magnitude of the reflection coefficient, $|S_{11}|$ is determined as the frequency is varied in the frequency band of interest. Figures 27-34 indicate that the bandwidth optimization in varying the substrate thickness can be achieved for approximate thickness of 7-8 cm. As thickness varies from 4 to 14 cm, smooth results in Figures 27-34 indicate that the same number of modes are excited. Table 3 outlines the numerical values for a such bandwidth optimization yielding BW=19.1 MHz. The bandwidth variation versus substrate thickness plotted in Figure 35 displays that optimization can be achieved.

The second phase of optimization is carried out by varying the dielectric constant of the substrate while keeping the thickness at its

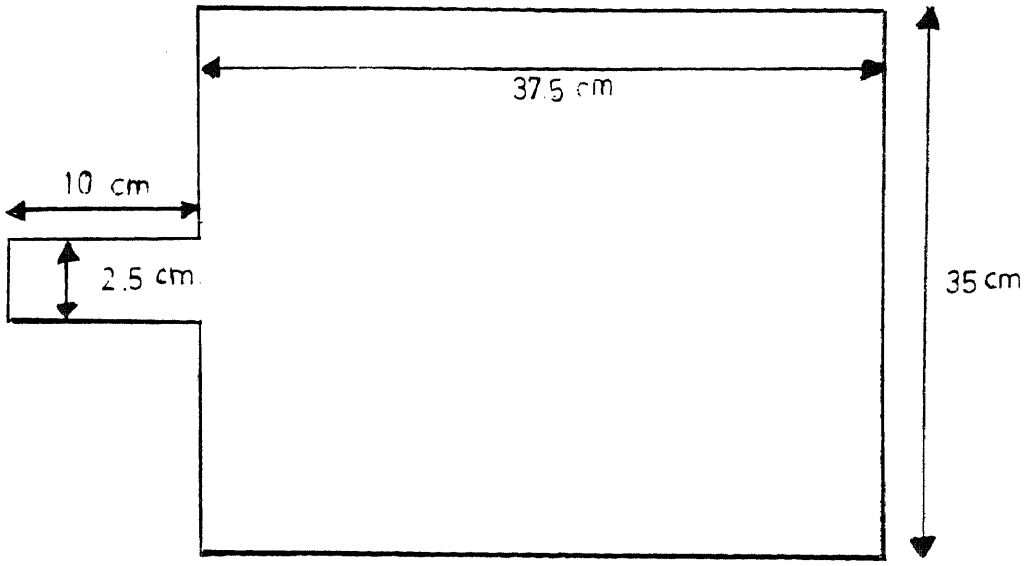

a) Patch geometry

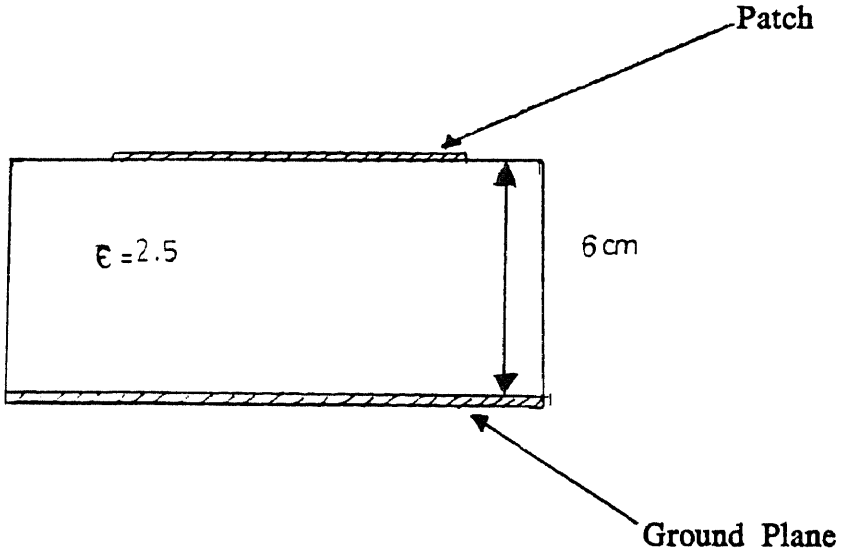

b) Crossectional view

Figure 26. Microstrip rectangular patch antenna for 400-500 MHz. frequency range.

Figure 27 Reflection coefficient performance versus substrate thickness for rectangular patch antenna over 4cm thick substrate BW=17.4 MHz

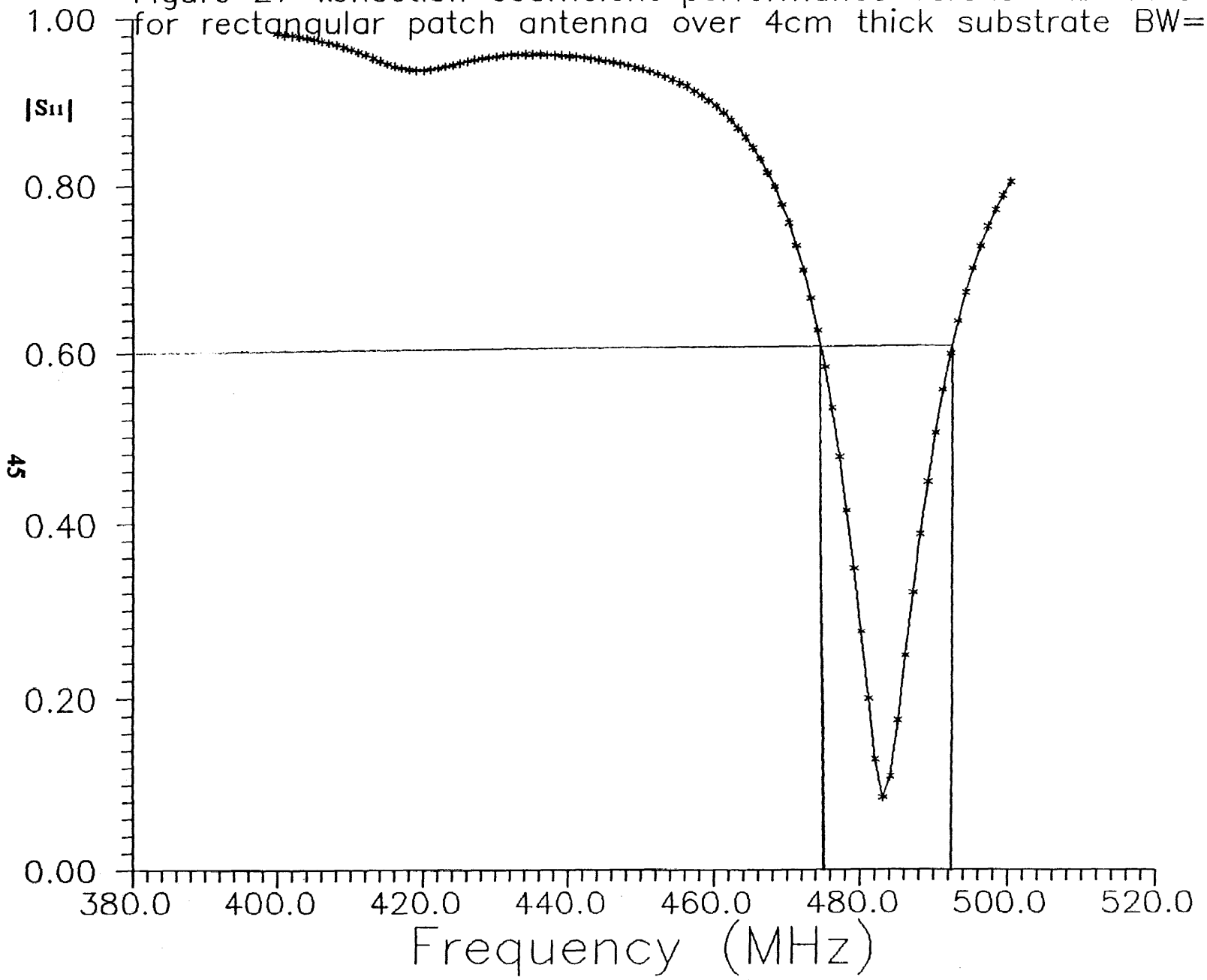

Figure 28 Reflection coefficient performance versus substrate thickness for rectangular patch antenna over 5cm thick substrate BW=18.3 MHz

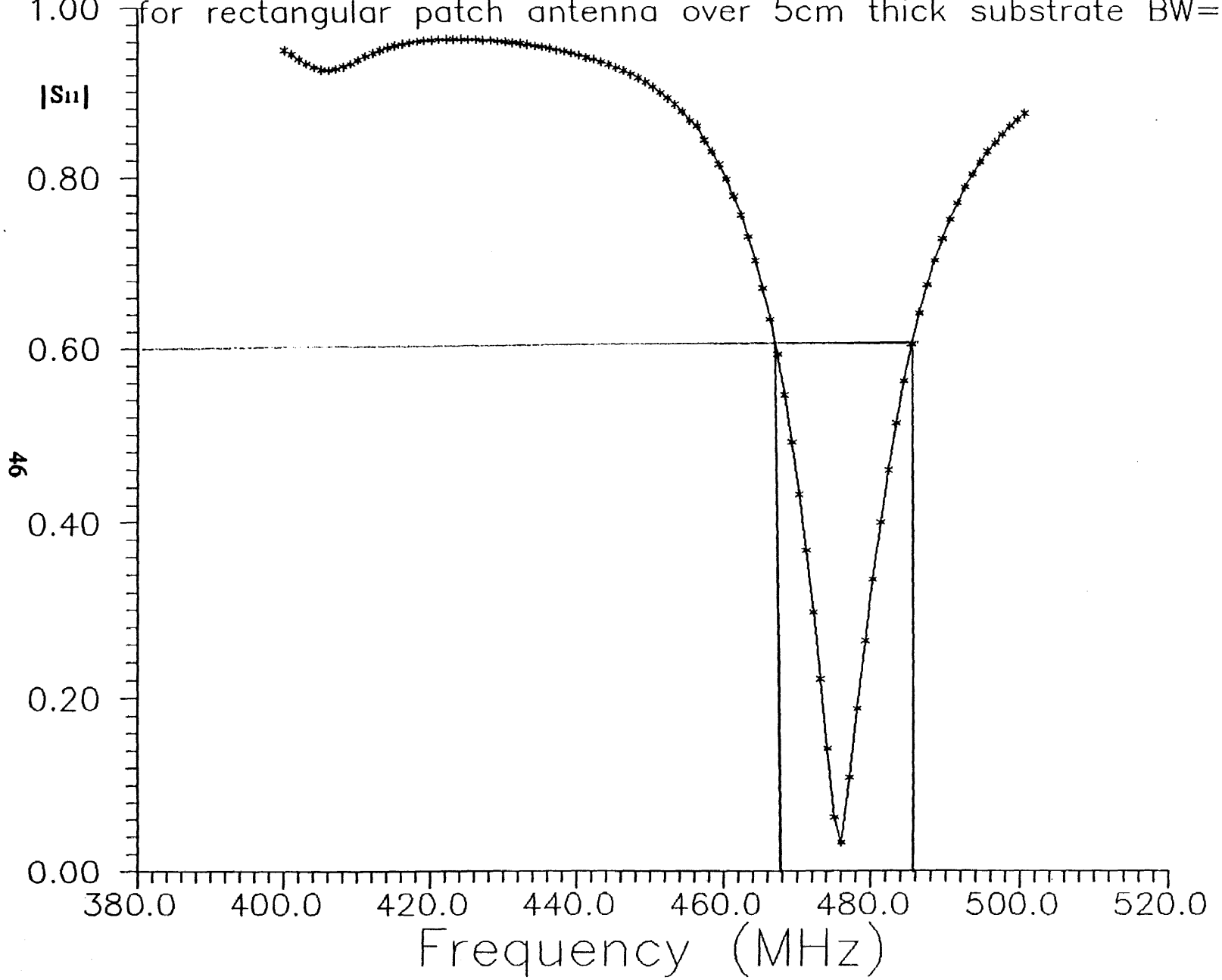

Figure 29 Reflection coefficient performance versus substrate thickness for rectangular patch antenna over 6cm thick substrate BW=18.8 MHz

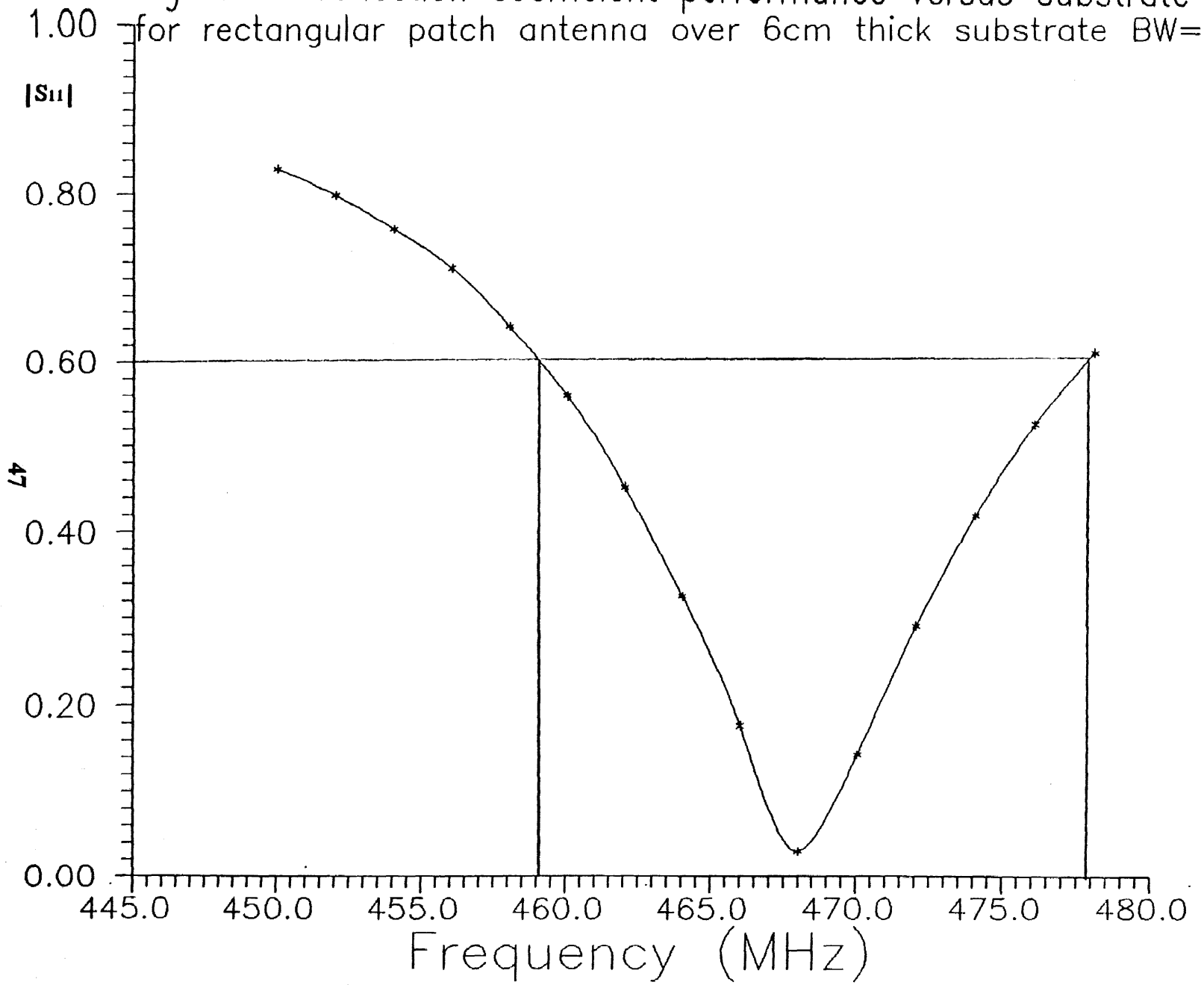

Figure 30 Reflection coefficient performance versus substrate thickness for rectangular patch antenna over 7cm thick substrate BW=19.1 MHz

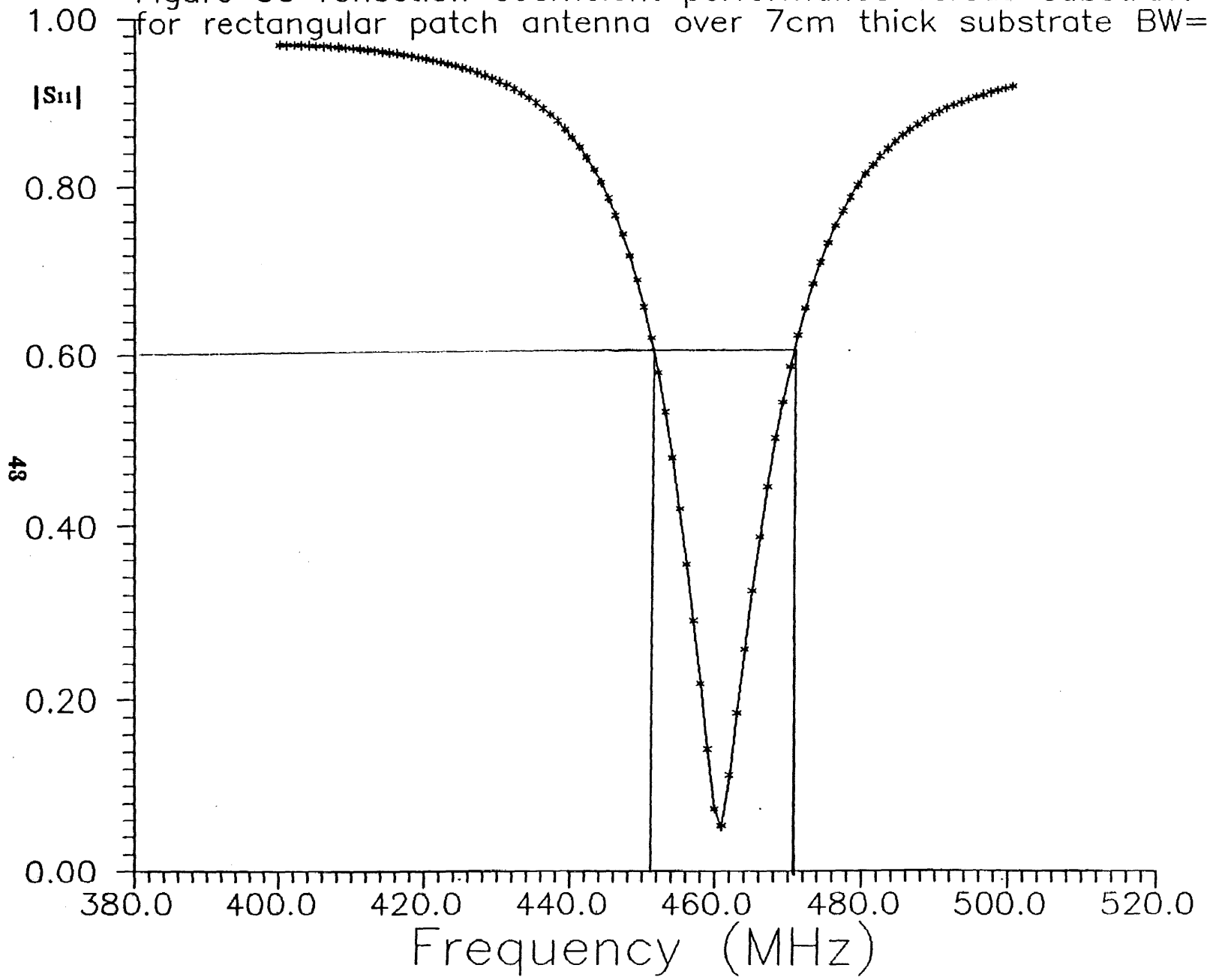

Figure 31 Reflection coefficient performance versus substrate thickness for rectangular patch antenna over 8cm thick substrate BW=19.1 MHz

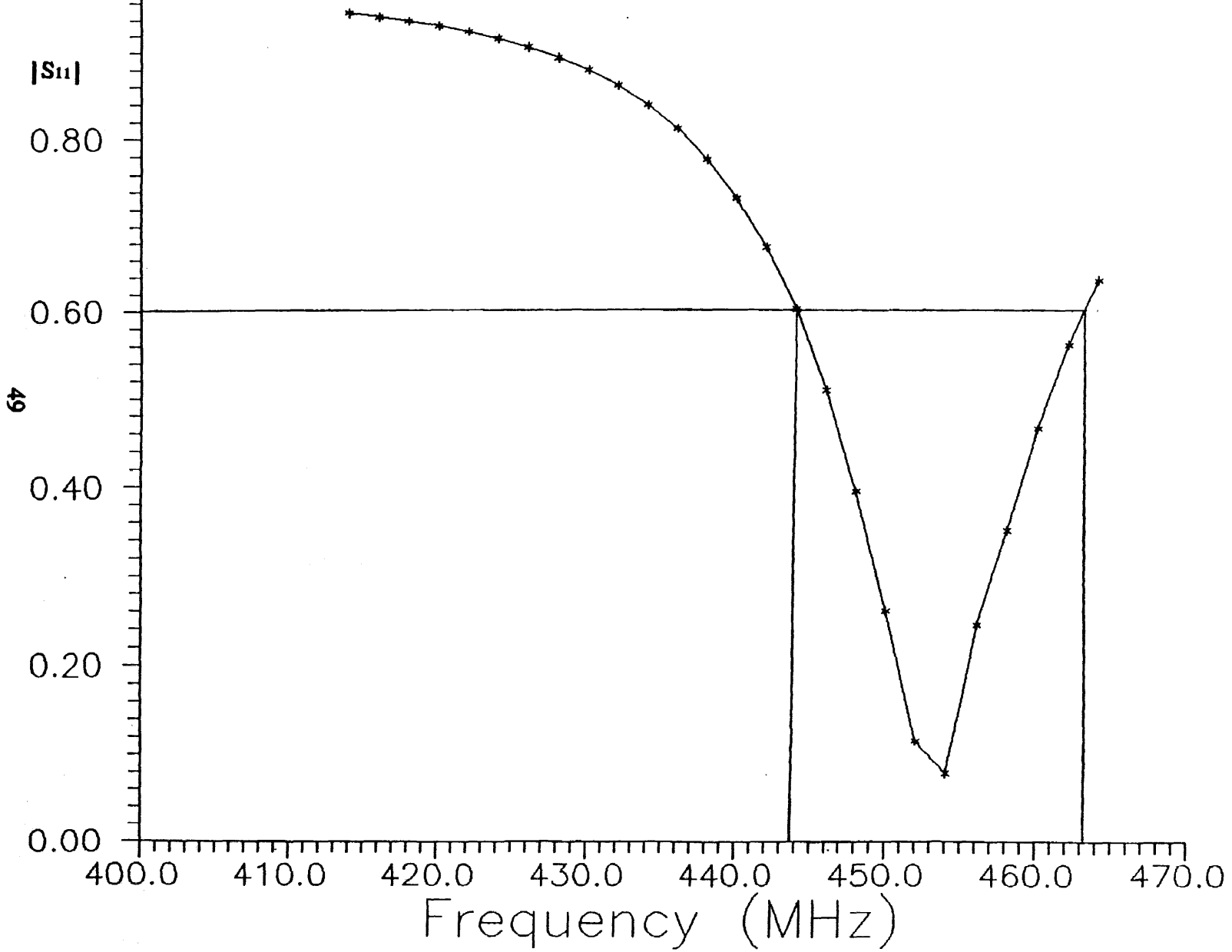

Figure 32 Reflection coefficient performance versus substrate thickness for rectangular patch antenna over 10cm thick substrate BW=18.5MHz

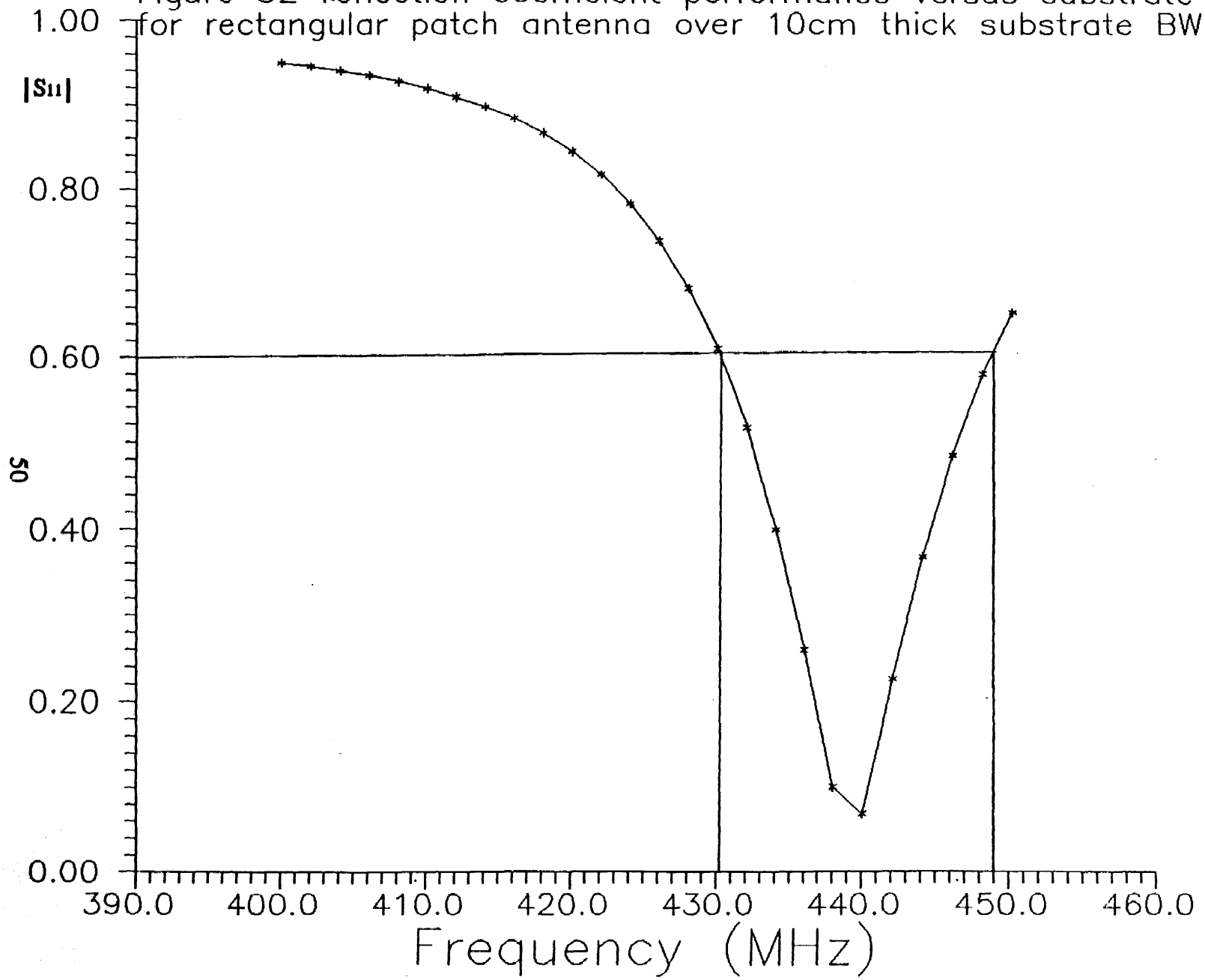

Figure 33 Reflection coefficient performance versus substrate thickness for rectangular patch antenna over 12cm thick substrate BW=17.5MHz

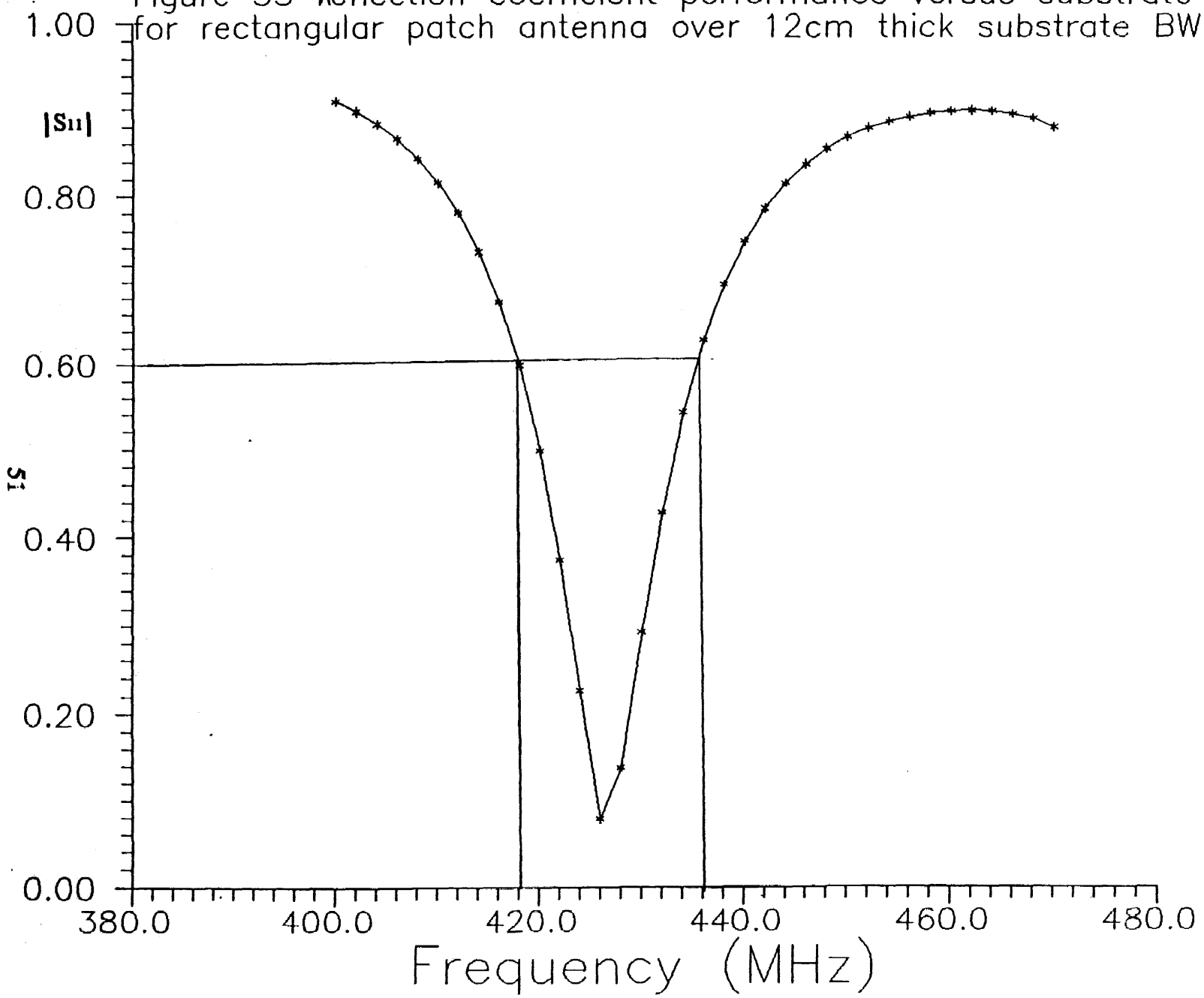

Figure 34 Reflection coefficient performance versus substrate thickness for rectangular patch antenna over 14cm thick substrate BW=16.3MHz

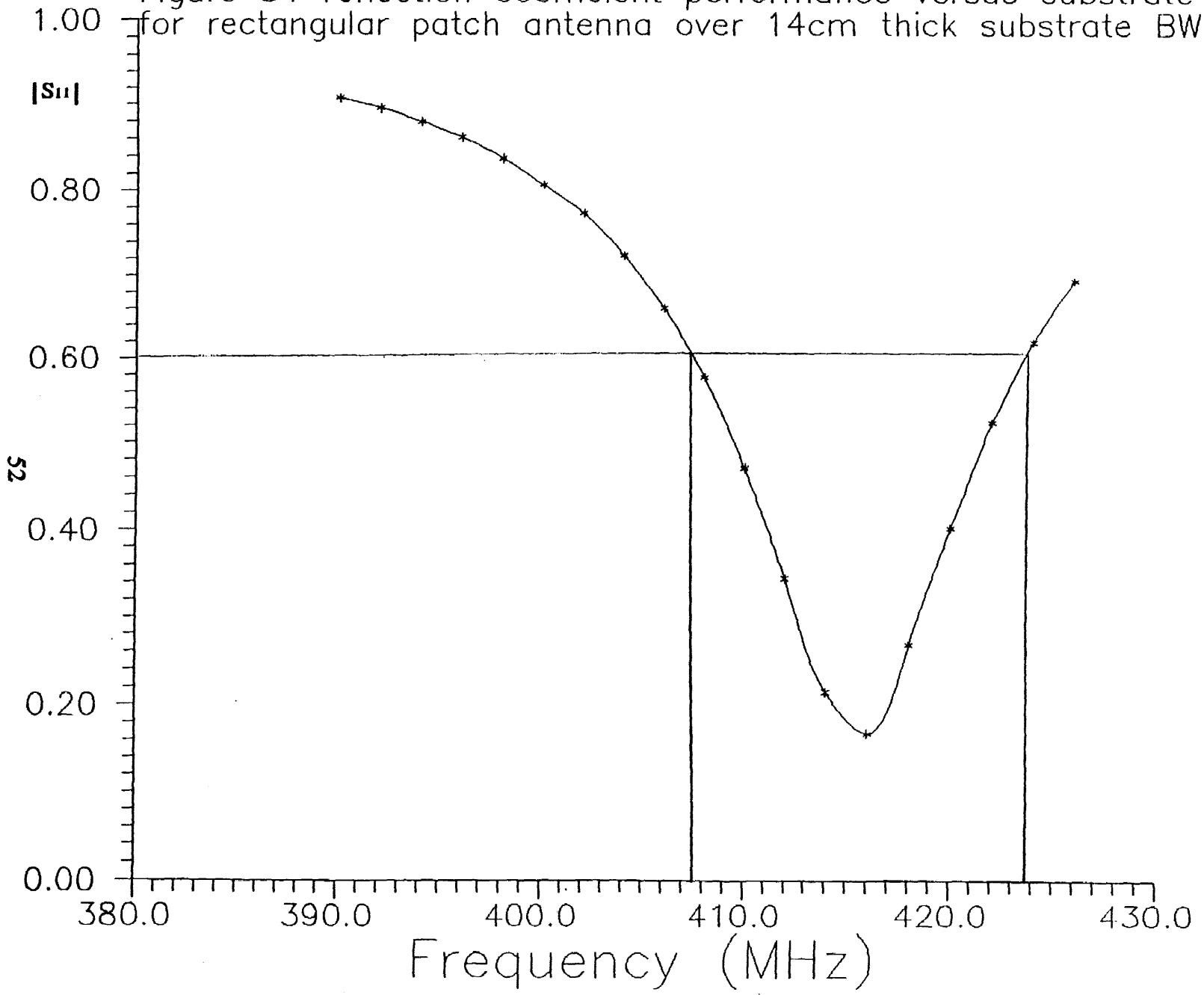

Thickness [cm]	Resonance Frequency [MHz]	h/λo	Bandwidth [MHz]	Plot Fig No
4	483	0.064	17.4	27
5	476	0.079	18.3	28
6	468	0.094	18.8	29
7	460	0.107	19.1	30
8	455	0.119	19.1	31
10	440	0.147	18.5	32
12	426	0.170	17.5	33
14	416	0.194	16.3	34

Table 3. Bandwidth optimization of the rectangular patch antenna in the 450 MHz band versus substrate thickness

Figure 35 Bandwidth performance versus normalized substrate thickness for rectangular patch antenna

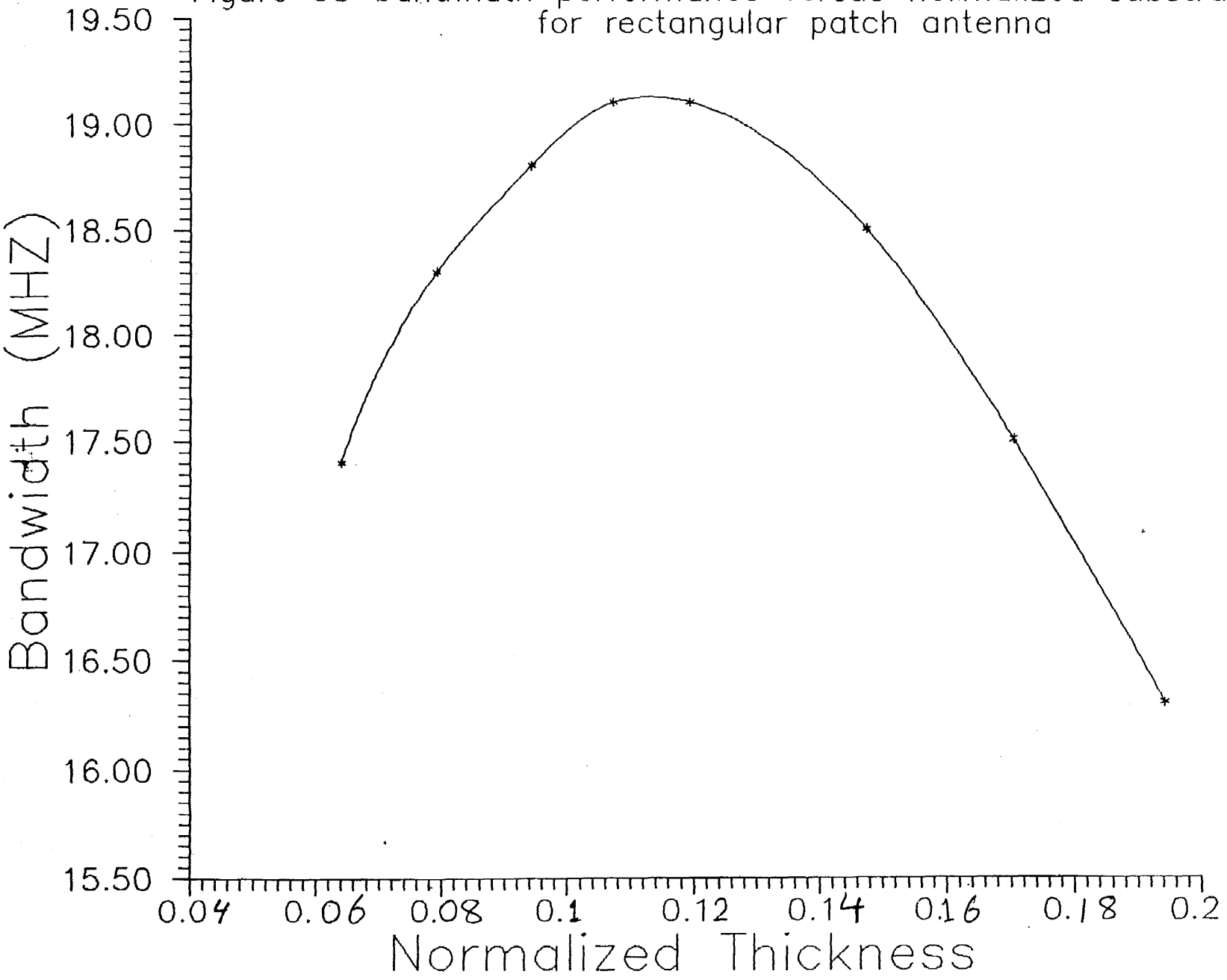

pre-optimized value. Keeping the substrate thickness at 7 cm, the relative dielectric constant of the substrate is varied from 2.5 to 1.5. Numerical response for $|S_{11}|$ versus frequency for various values of ε_r is presented in Figures 36-41. Numerical results indicate that for the tolerable maximum $|S_{11}|=0.6$, the bandwidth optimization is achieved when $\varepsilon_r=1.9$. Also it is observed that as ε_r is decreased the sharpness of the resonance tends to decrease, which is quite distinct if Figures 36 and 41 are compared. The bandwidths obtained in this process are included in Table 4 and plotted in Figure 42, yielding the maximum value of BW=25.4 MHz. Above results do not satisfy the requirements set for the practical operation. Hence, it is possible to improve them by investigating other patch geometries.

Circular Patch Antenna

The extension of the analysis from rectangular patch to a circular patch antenna, leads to improved bandwidth characteristics. Furthermore, multiport excitation of circular antennas yield circularly polarized radiation field if proper phase relationship exists at multiple inputs [7]. When compared to the rectangular patch, a circular microstrip antenna on the same size substrate yields a better bandwidth. The feed structure for the circular patch is shown in Figure 43, where the feed is located on a different level than the patch. The connection between the two levels is achieved by introducing a via from the feed line to the contact location on the patch. Results in Figure 44, yield an approximate BW=35.5 MHz for a circular patch. The

Figure 36 Reflection coefficient performance versus dielectric constant for a dielectric constant=2.5, BW=19.1 MHz

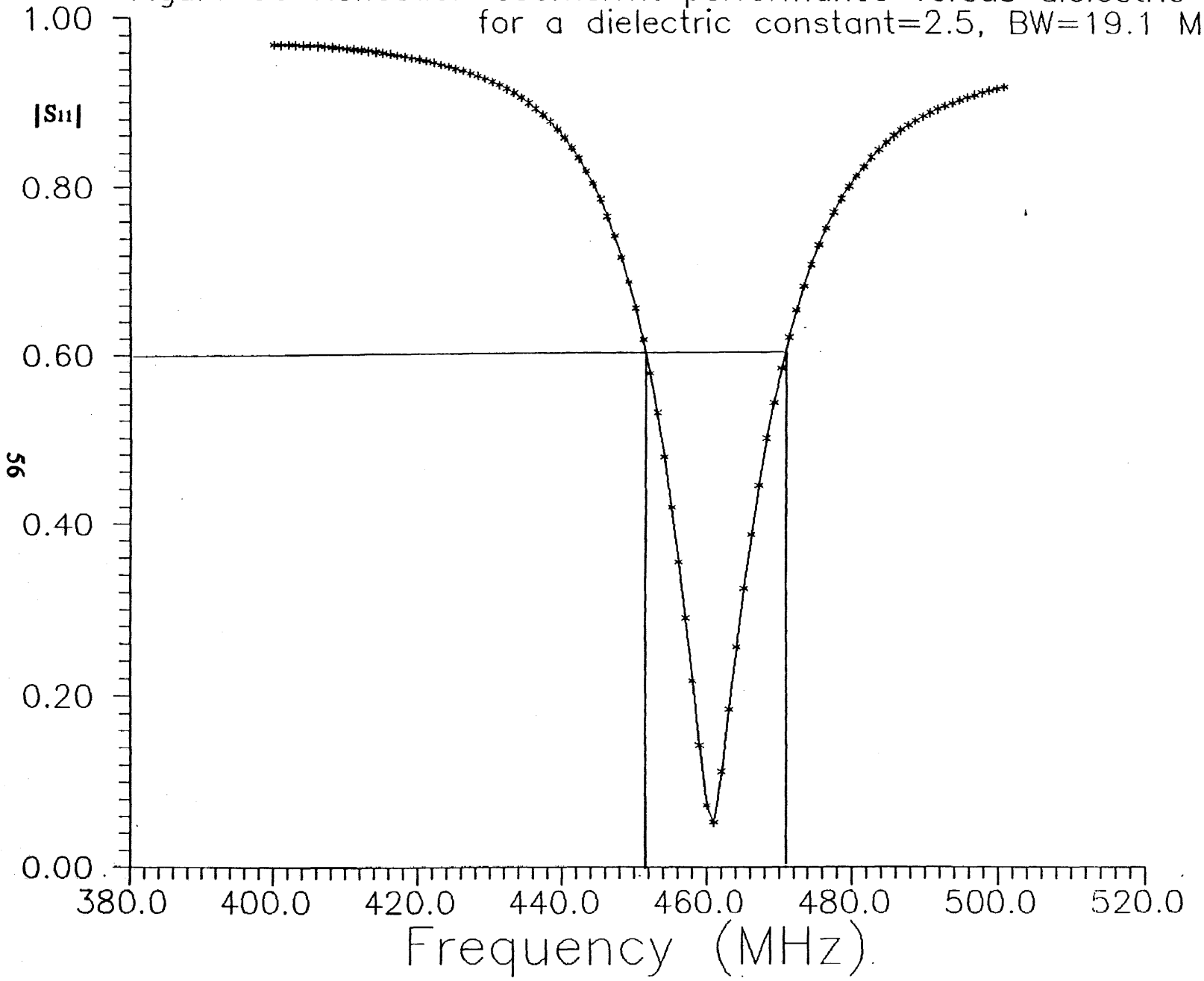

Figure 37 Reflection coefficient performance versus dielectric constant for a dielectric constant=2.2, BW=22.5 MHz

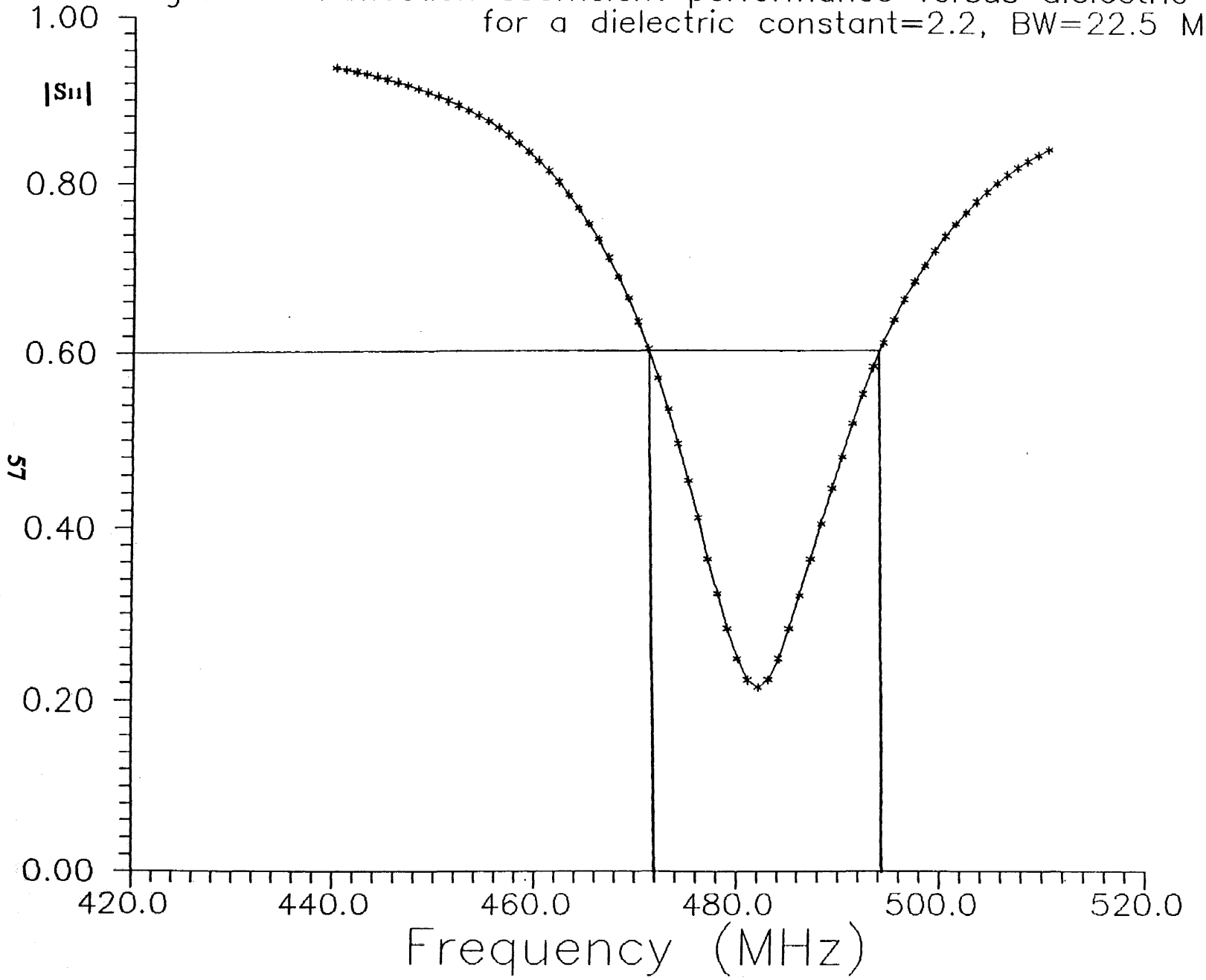

Figure 38 Reflection coefficient performance versus dielectric constant for a dielectric constant=2.1, BW=23.5 MHz

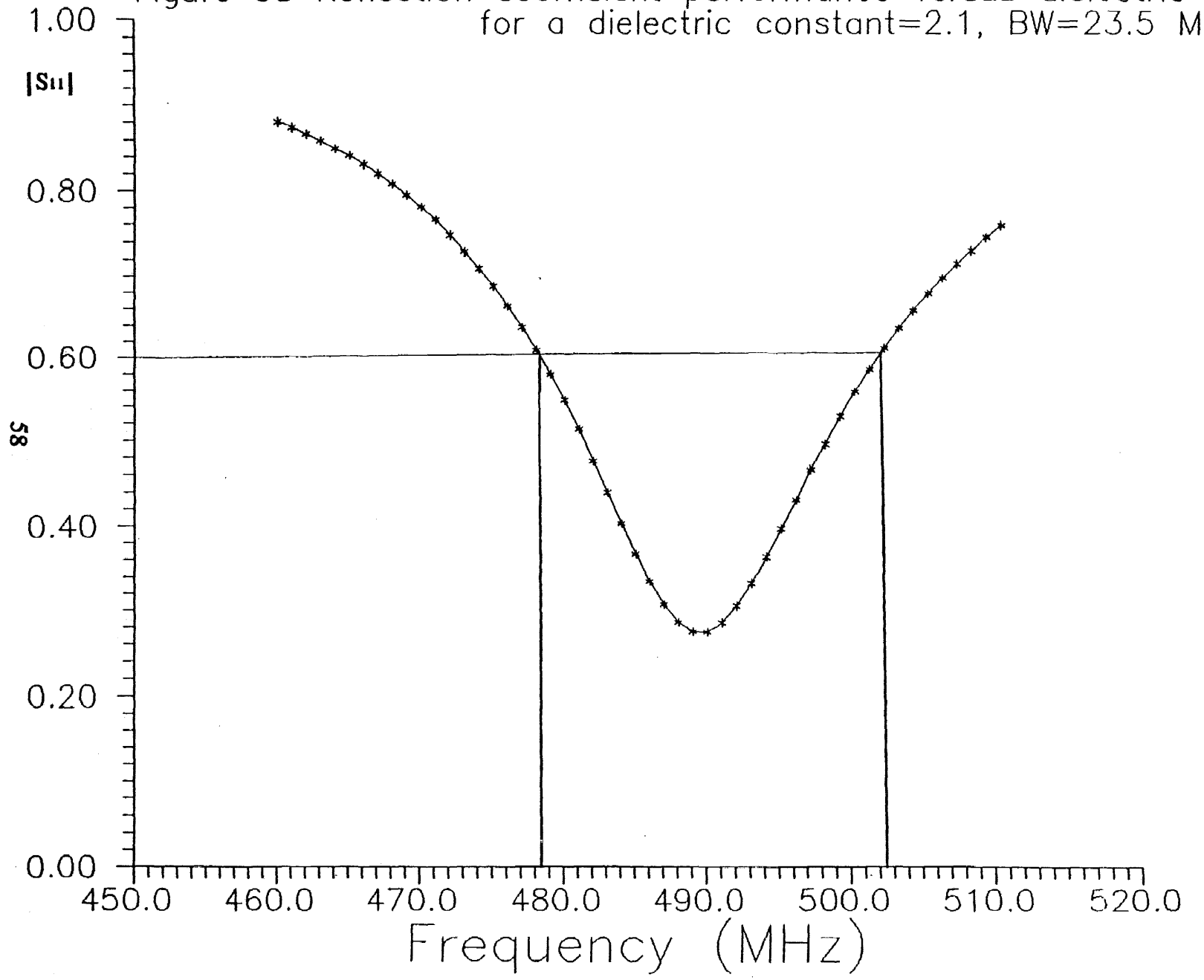

Figure 39 Reflection coefficient performance versus dielectric constant for a dielectric constant=2.0, BW=24.2 MHz

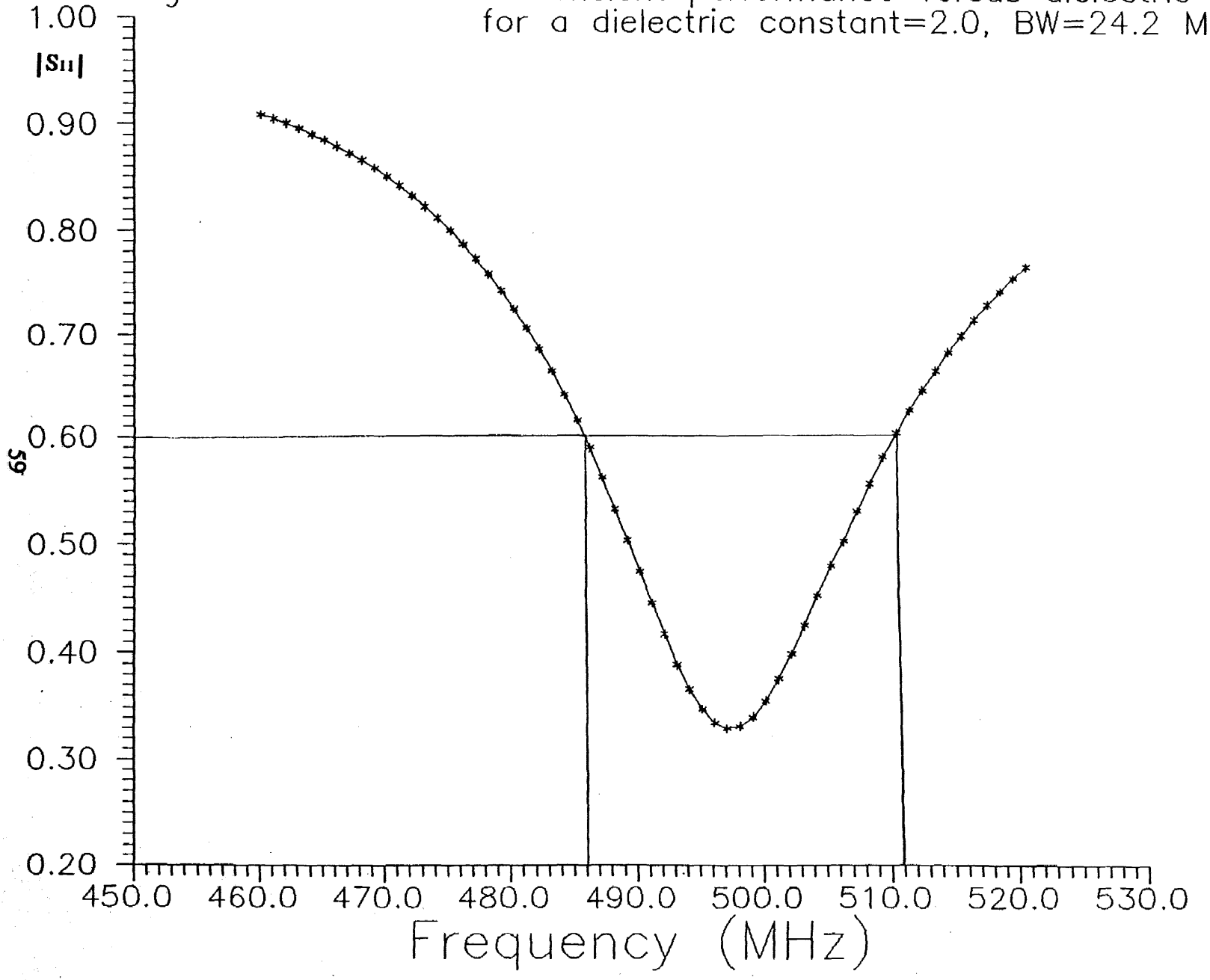

Figure 40 Reflection coefficient performance versus dielectric constant for a dielectric constant=1.9, BW=25.4 MHz

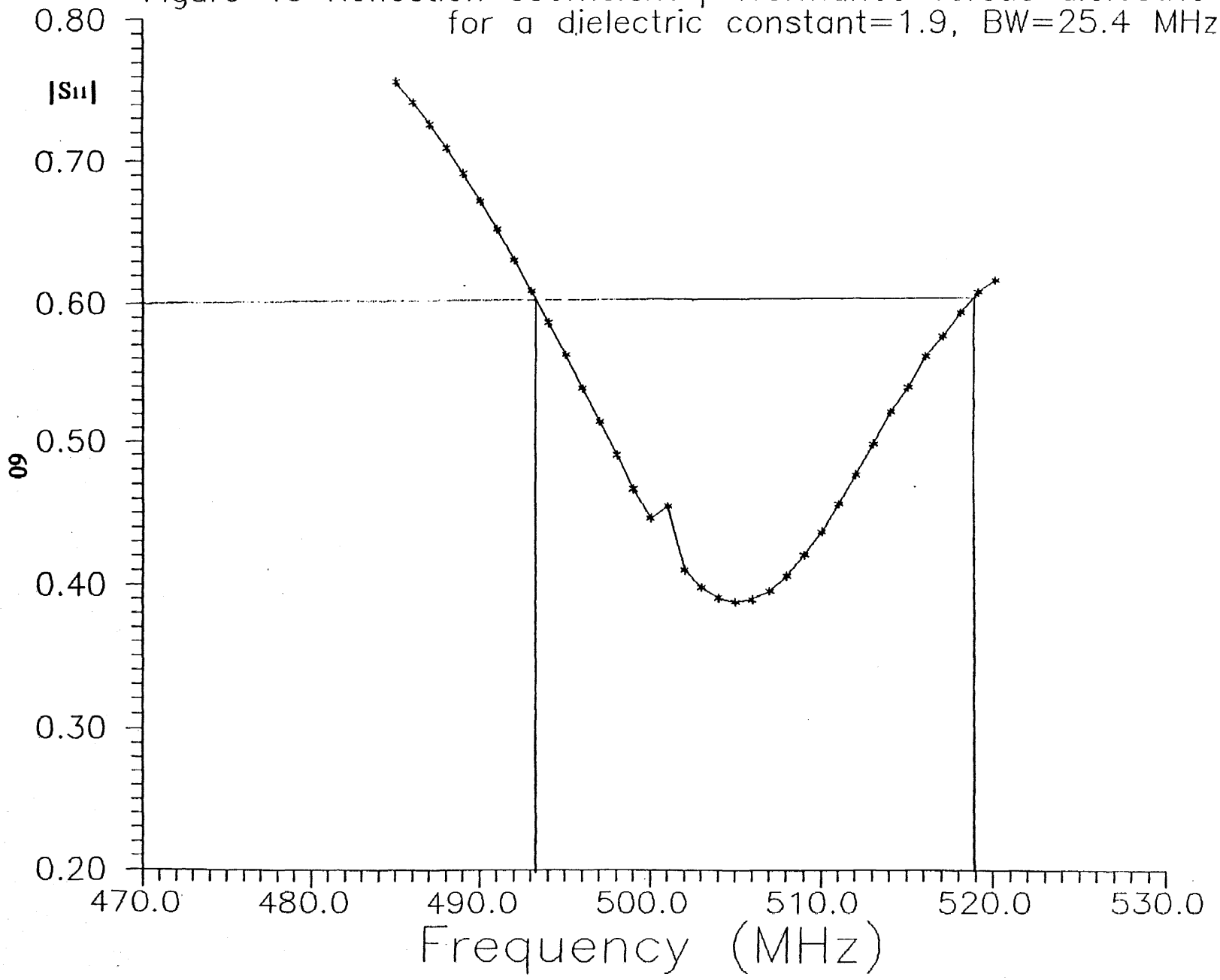

Figure 41 Reflection coefficient performance versus dielectric constant for a dielectric constant=1.5, BW=12.0 MHz

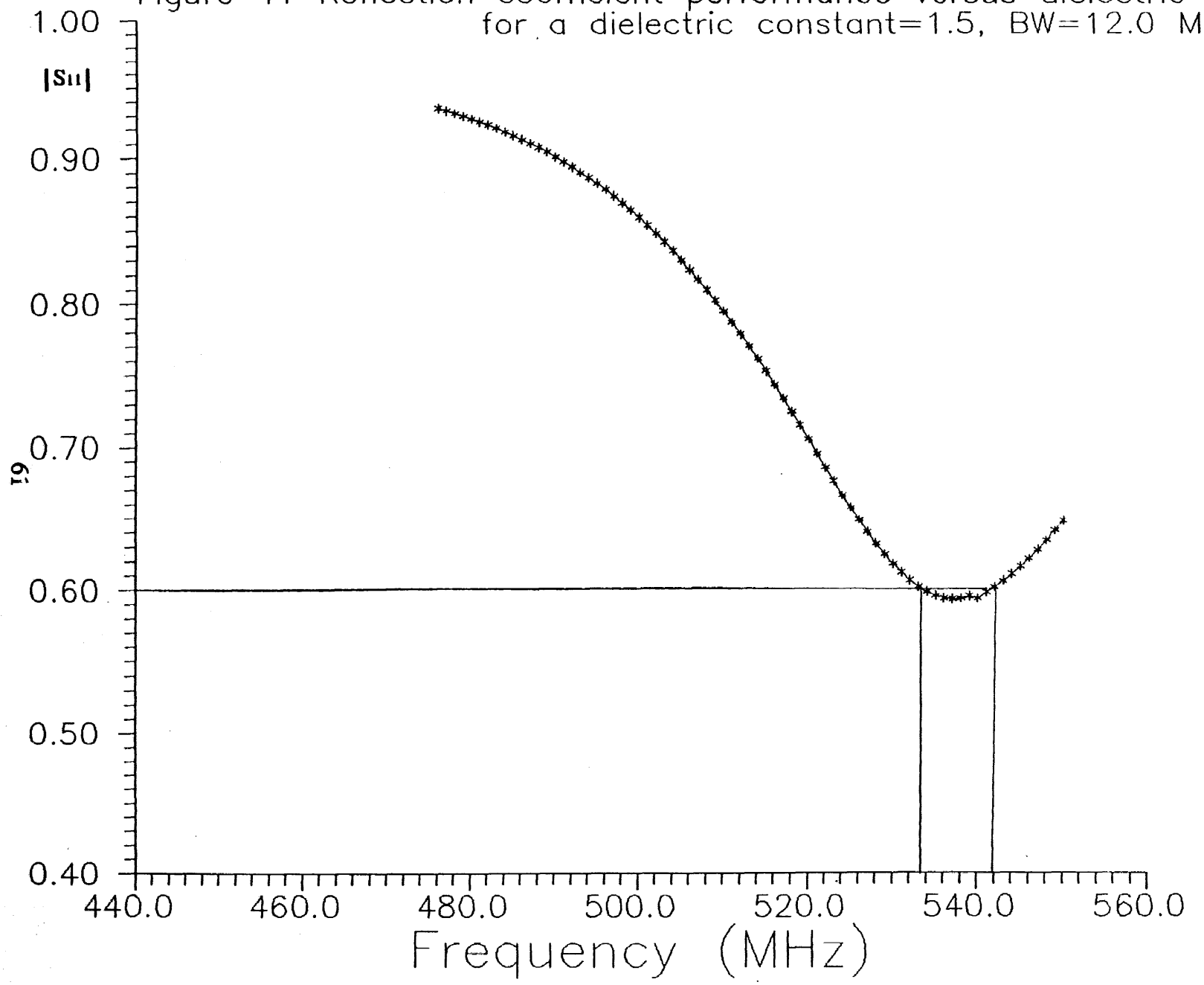

Dielectric constant	Bandwidth [MHz]	Plot Fig No
2.5	19.1	36
2.2	22.5	37
2.1	23.5	38
2.0	24.2	39
1.9	25.4	40
1.5	12.0	41

Table 4. Bandwidth optimization of the rectangular patch antenna over a 7 cm thick substrate versus dielectric constant

Figure 42 Bandwidth performance versus dielectric constant for a rectangular patch antenna

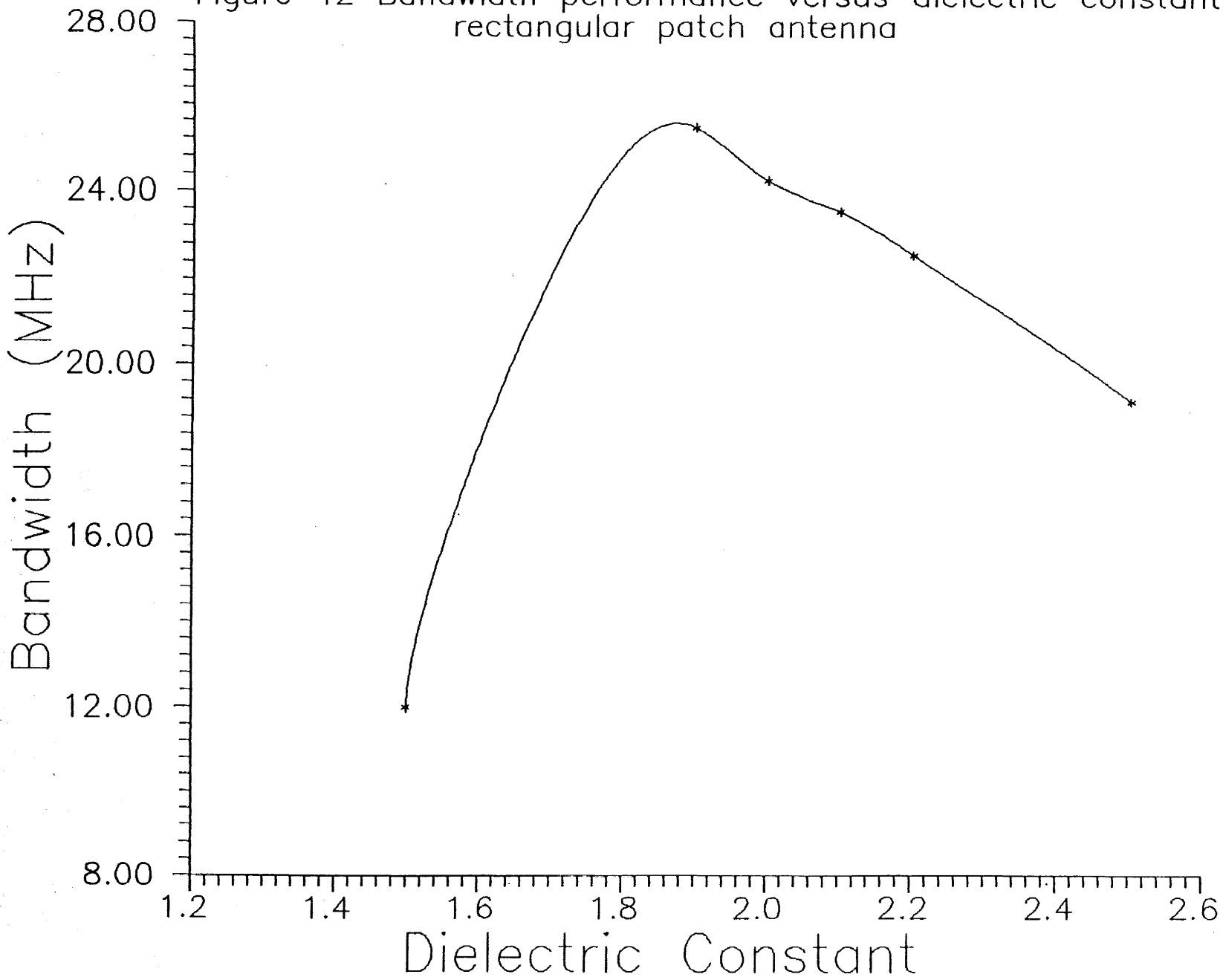

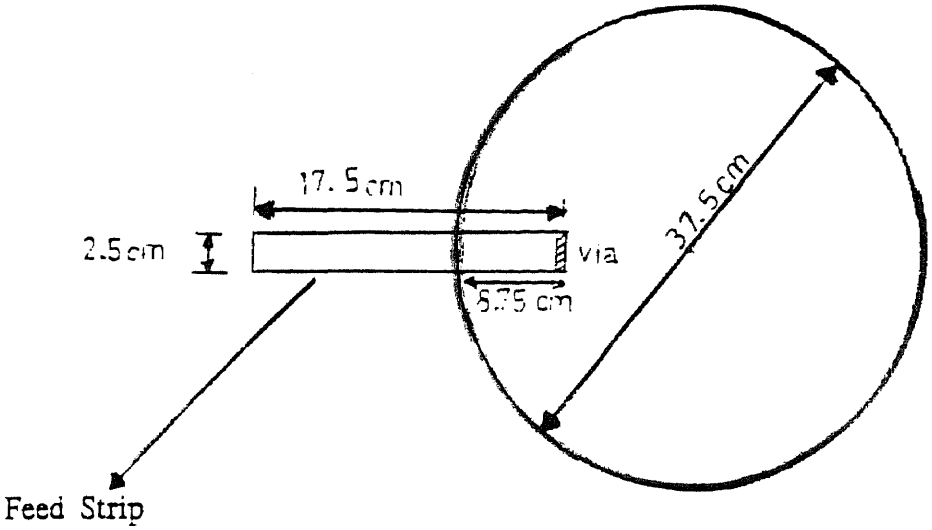

a) Circular patch with feed line.

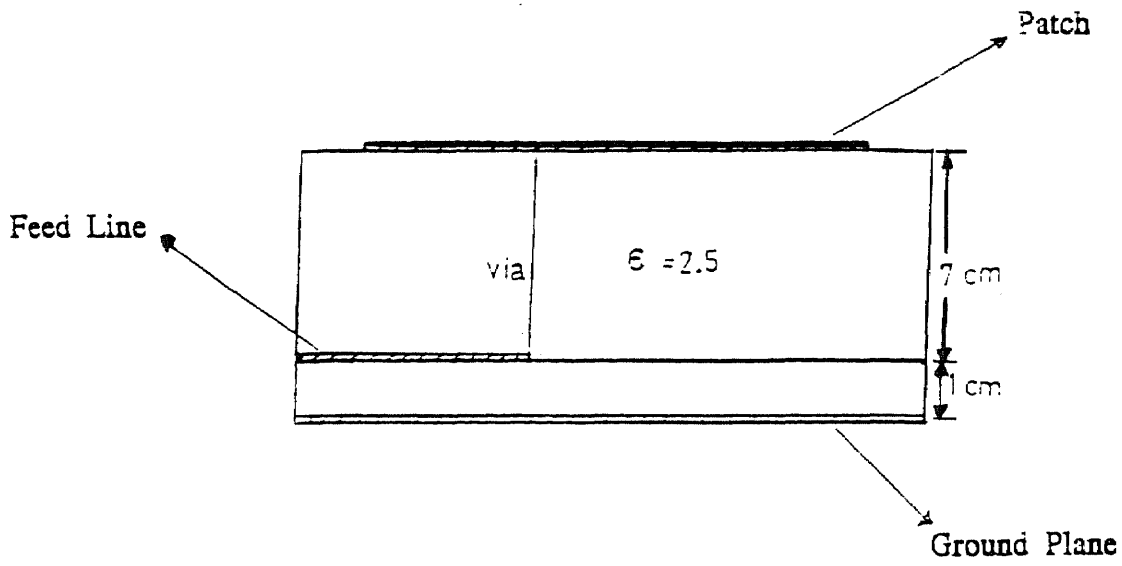

b) Crossectional view

Figure 43. Circular microstrip patch antenna.

Figure 44 Reflection coefficient performance versus frequency for a circular patch antenna BW = 35.5 MHz

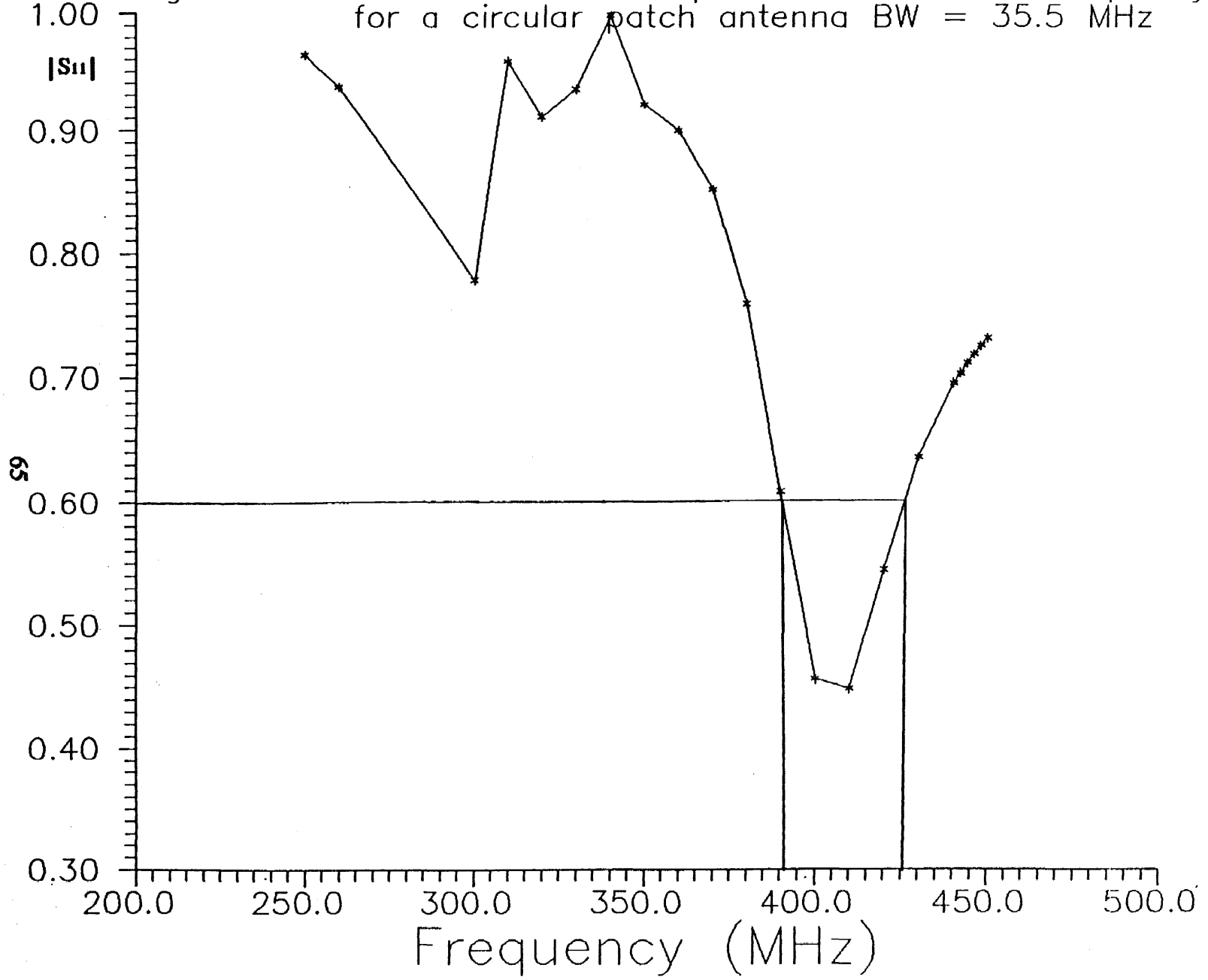

comparable rectangular patch of similar dimensions yields only the optimized value of BW=19.1 MHz (Figure 31).

Optimization of the Annular Ring Patch Antenna

Ring structure in the microstrip antenna geometries tend to yield smaller Q-factor, higher gain and larger bandwidth [8]. If the hole is opened within the circular patch, it results in less stored energy and hence more radiation.The annular ring geometry shown in Figure 45 is studied numerically over the substrate configuration used in Figure 43. The reflection coefficient performance in Figure 46 yields results with a kind of obstacle in the form of a lobe in the middle of the band. The lobe in the pattern can be explained due to the presence of internal resonances within the annular structure and their modal contribution to the overall response. In order to improve its performance, the parameters needed to be optimized are the relative dielectric constant of the substrate, relative radii of the annular ring and the feed location.

If the relative dielectric constant of the substrate is decreased, there is a substantial drop in the lobe level in the band of interest resulting in improved bandwidth performance. Such a plot is given in Figure 47 where $\varepsilon_r = 1.8$ while the annular ring dimensions and other parameters were kept fixed. Variation of the inner diameter of the annular ring patch yielded approximate optimization for a value 22.5 cm (Figure 48). Further decrease in ε_r to 1.6 from 1.8 did not produce a significant effect in the lobe level (Figure 49).

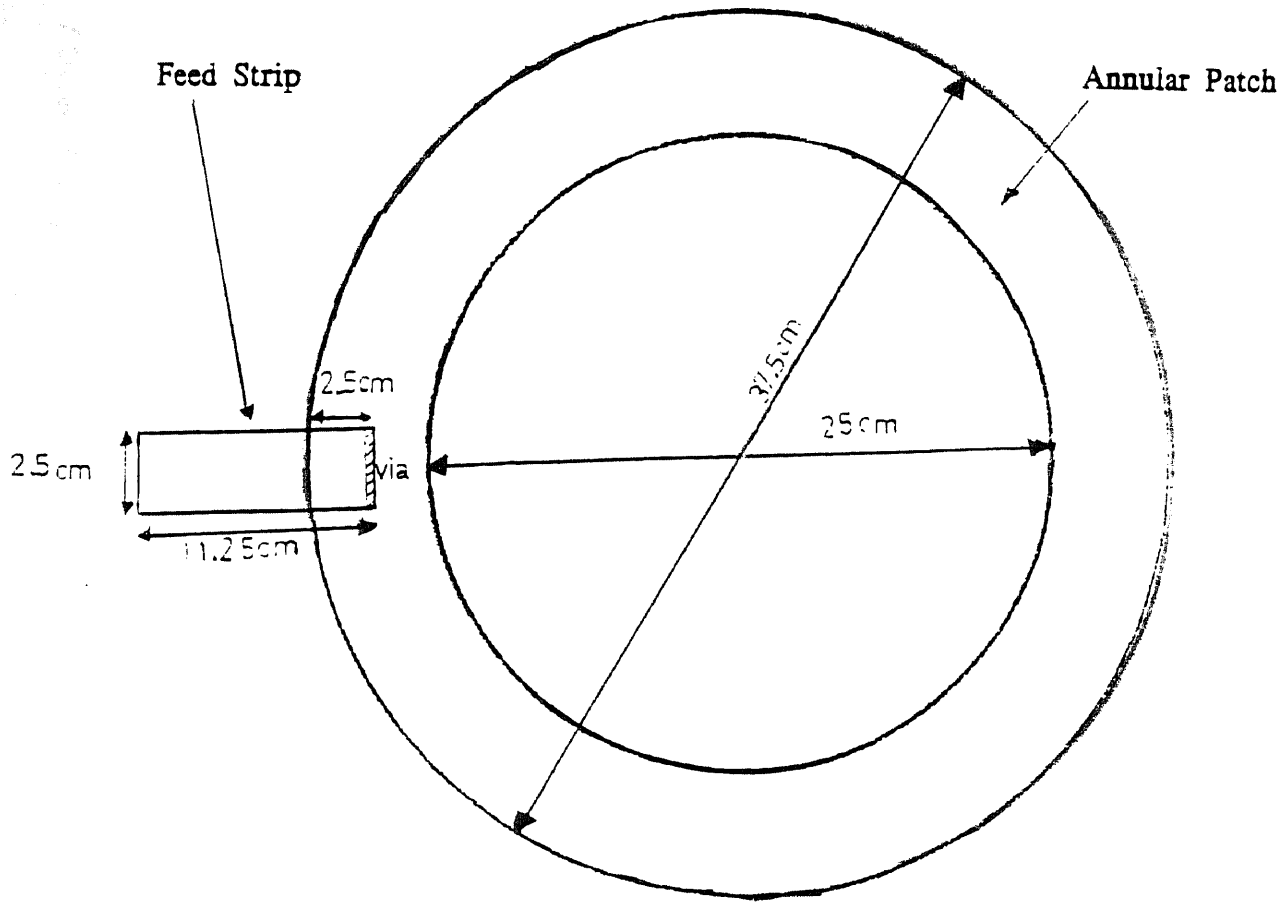

Figure 45. The annular ring patch geometry

Figure 46 Reflection coefficient performance versus frequency for annular patch antenna (Dielectric constant=2.5)

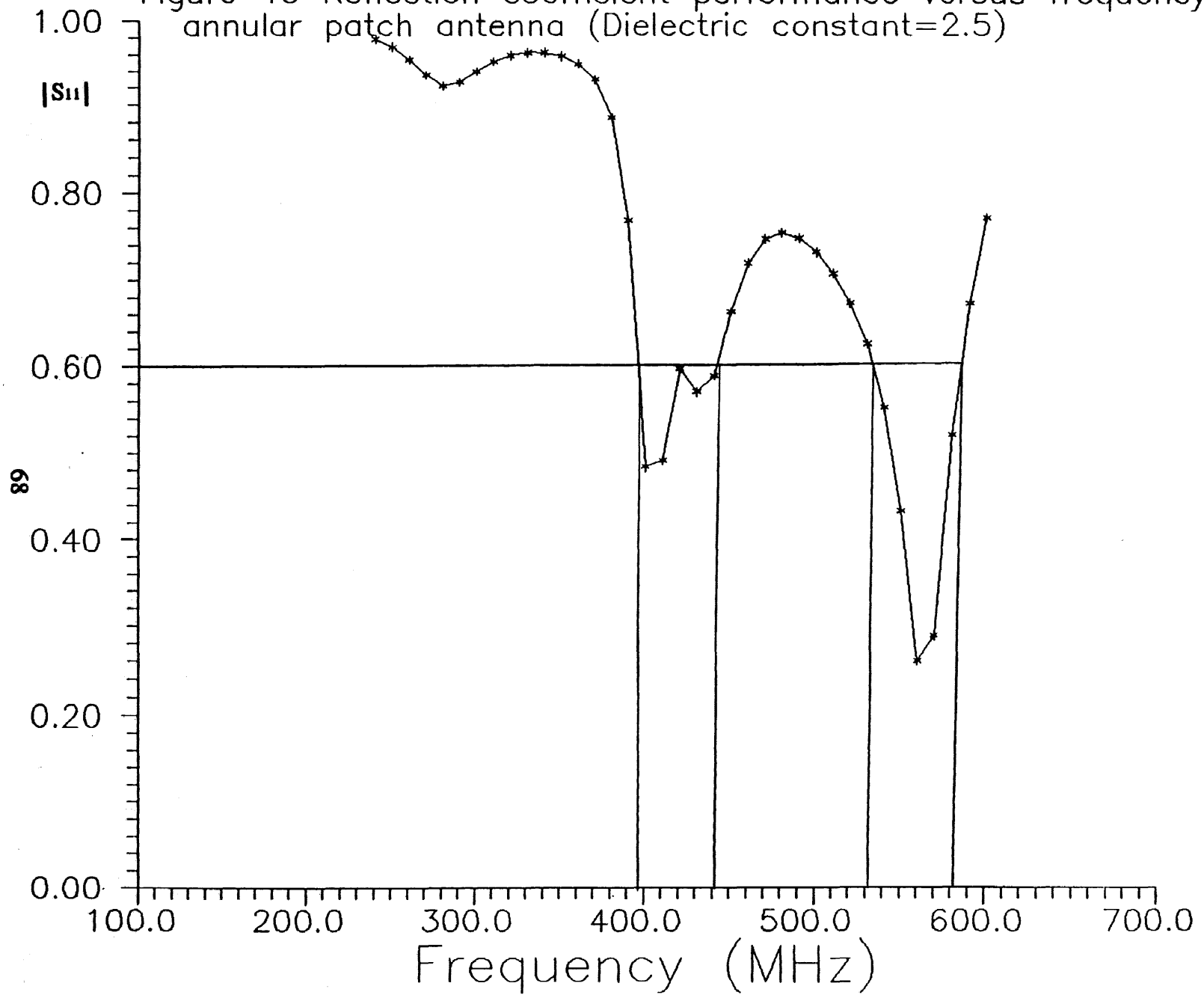

Figure 47. Reflection coefficient performance versus frequency for annular patch antenna (Dielectric constant=1.8)

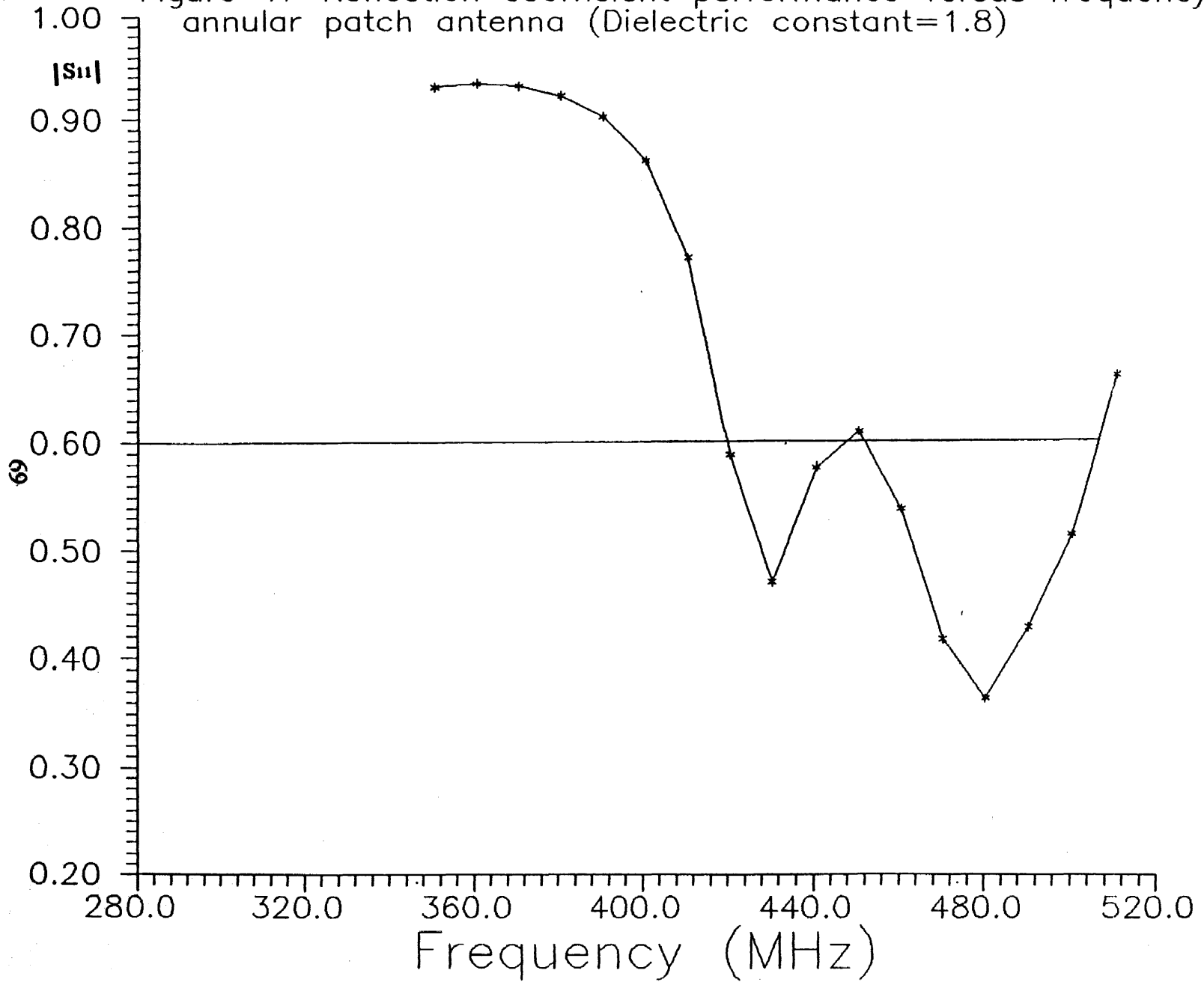

Figure 48 Reflection coefficient performance versus frequency for annular patch antenna with smaller hole (Dielectric Cons.=1.8)

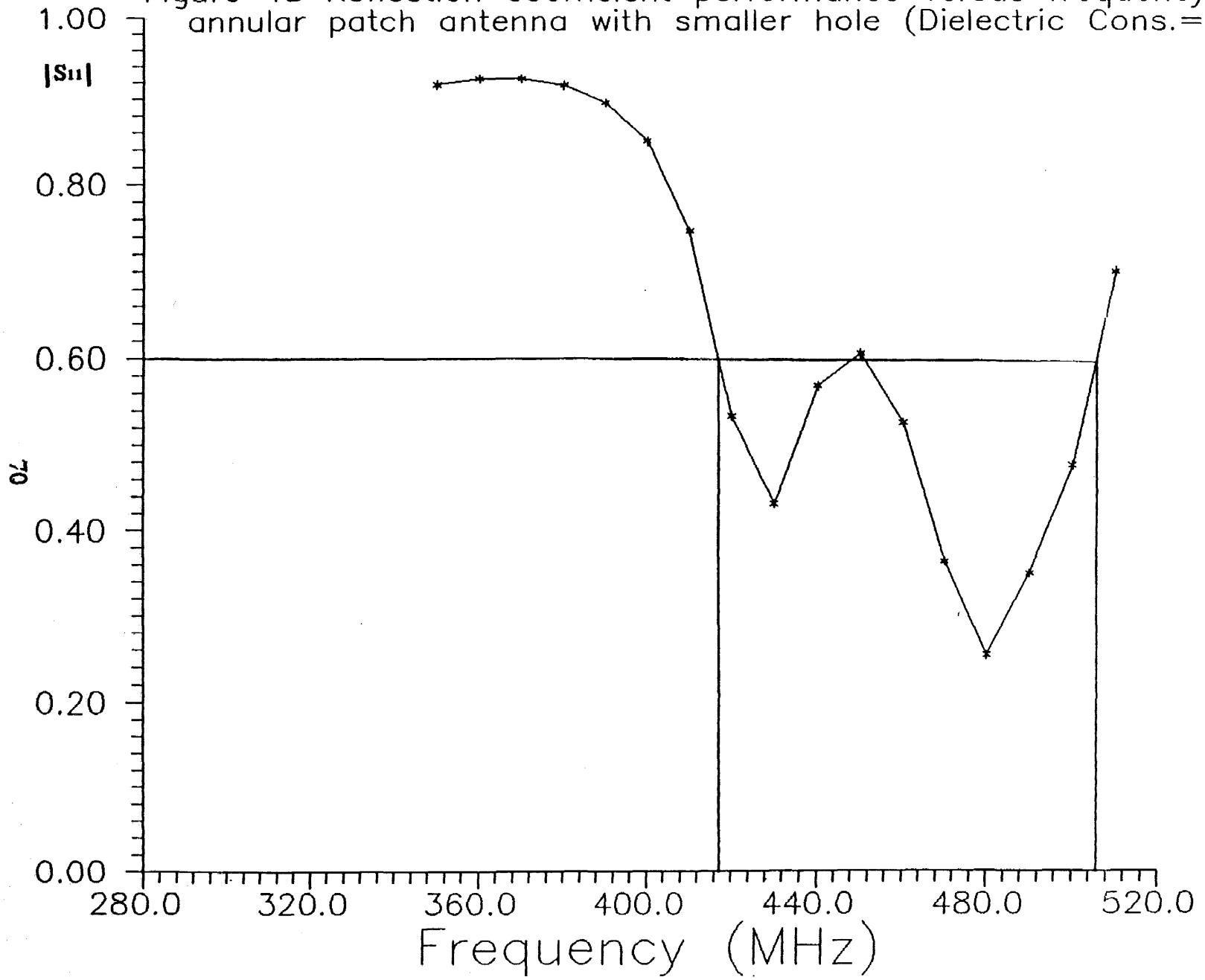

Figure 49 Reflection coefficient performance versus frequency for annular patch antenna with smaller hole (Dielectric Cons.=1.6)

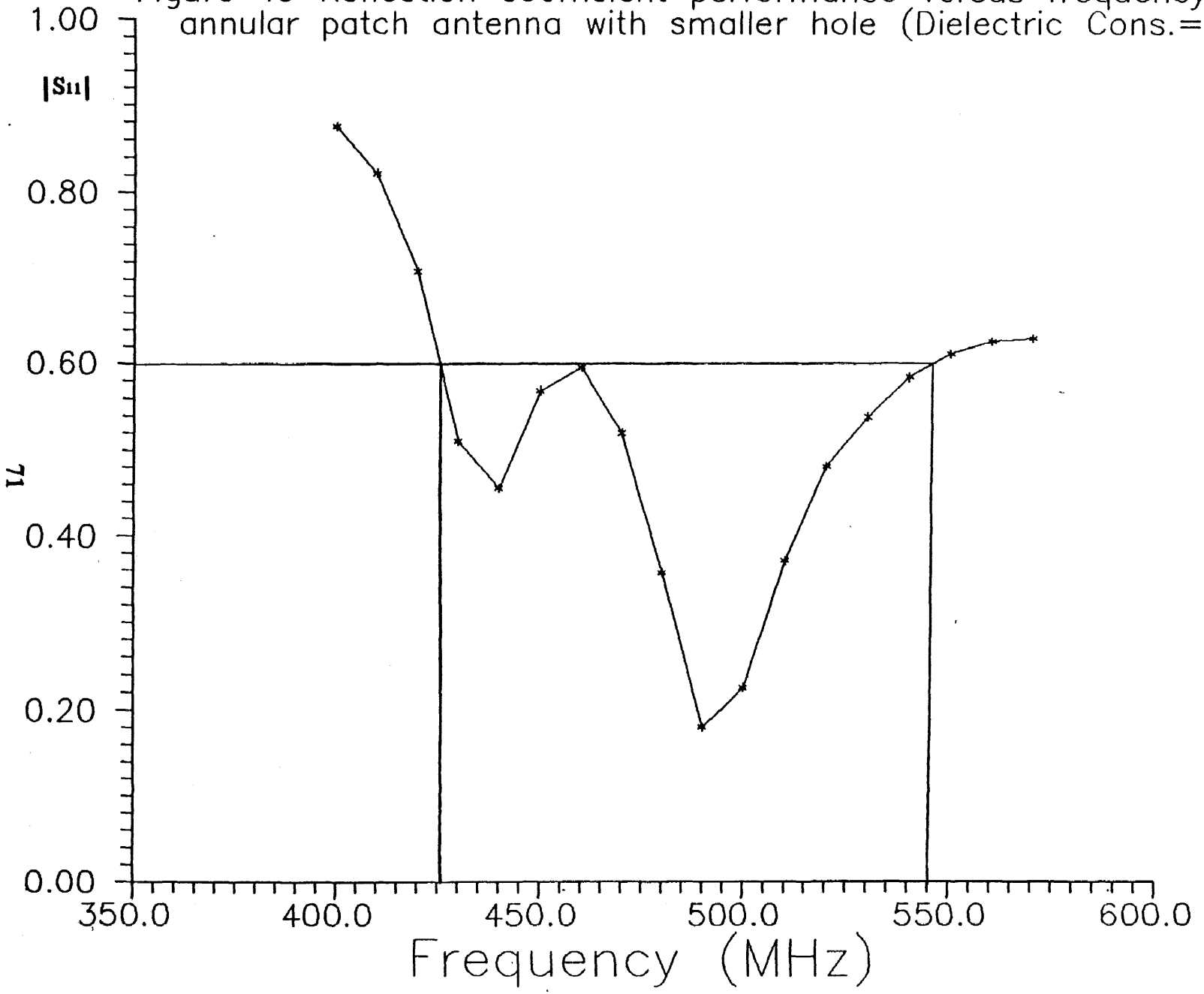

The location of the feed contact along the annular ring leads to optimization of the bandwidth performance in itself. Typical geometry (Figure 50) that produced the optimized performance (Figure 51) yielded BW $\sim$ 146 MHz. Even if the maximum tolerable reflection coefficient magnitude is assumed to be 0.4, the retained bandwidth still exceeds 80 MHz. This corresponds to VSWR $\cong$ 2.3.

Circular Polarization

There exists extensive literature [7] on possible feeding configurations to obtain circularly polarized (CP) fields radiated from the microstrip antennas. An efficient approach to obtain circular polarization is to apply feed structure at two ports, where ports are excited with 90° phase shift. This is applicable to an annular ring and previously optimized geometry is now extended to accommodate such a double feed location as shown in Figure 52. Since there are two ports involved in this particular geometry, there are four different S-parameters involved. Rather than plotting individual parameters, an approximate estimate for radiated power (neglecting internal losses) is suggested as

$$P_{rad} \cong \frac{P_{in}}{2} [(1-|S_{11}|^2-|S_{12}|^2)+(1-|S_{22}|^2-|S_{21}|^2)] \qquad (25)$$

The above expression is determined numerically and plotted in Figure 53. If more than 60% of the power is assumed to radiate, the resulted bandwidth is determined to be over 150 MHz.

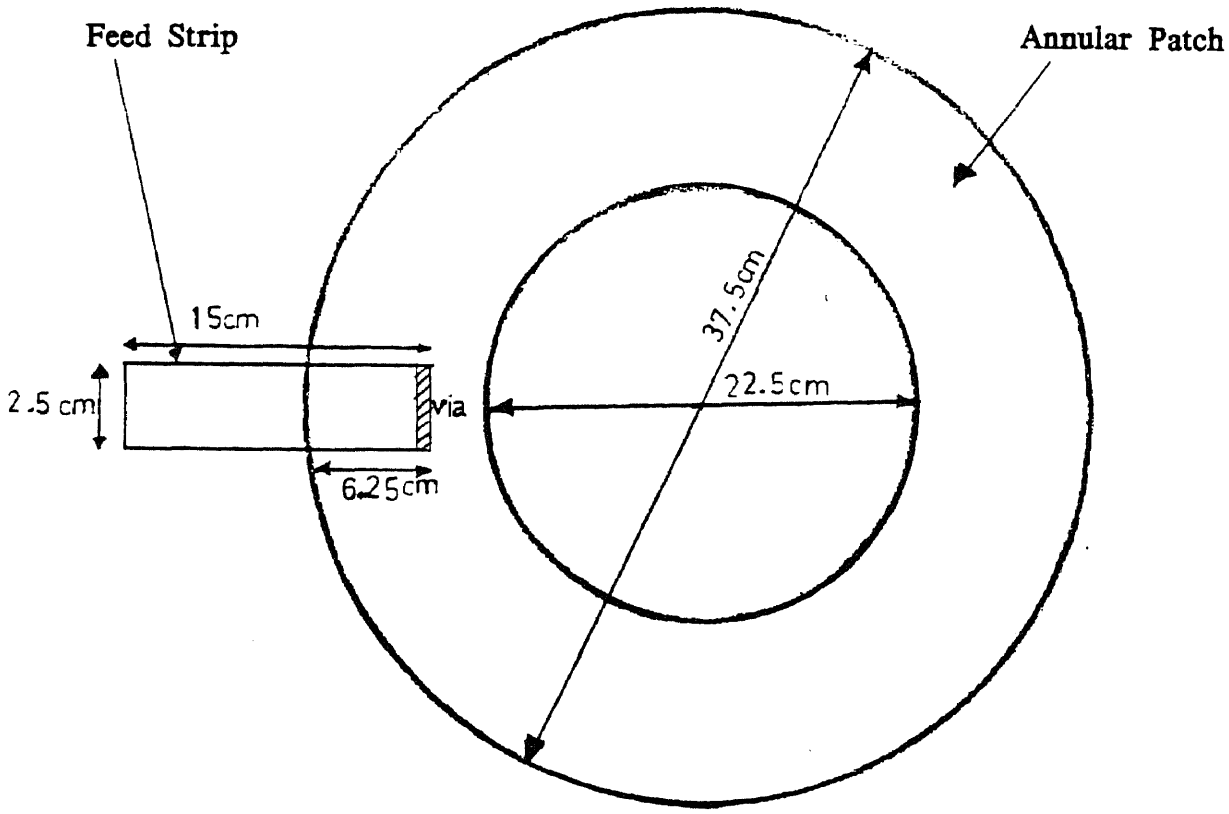

Figure 50. The optimized feed location for the annular ring patch geometry.

Figure 51 Optimized performance versus frequency for annular ring patch antenna BW = 146 MHz

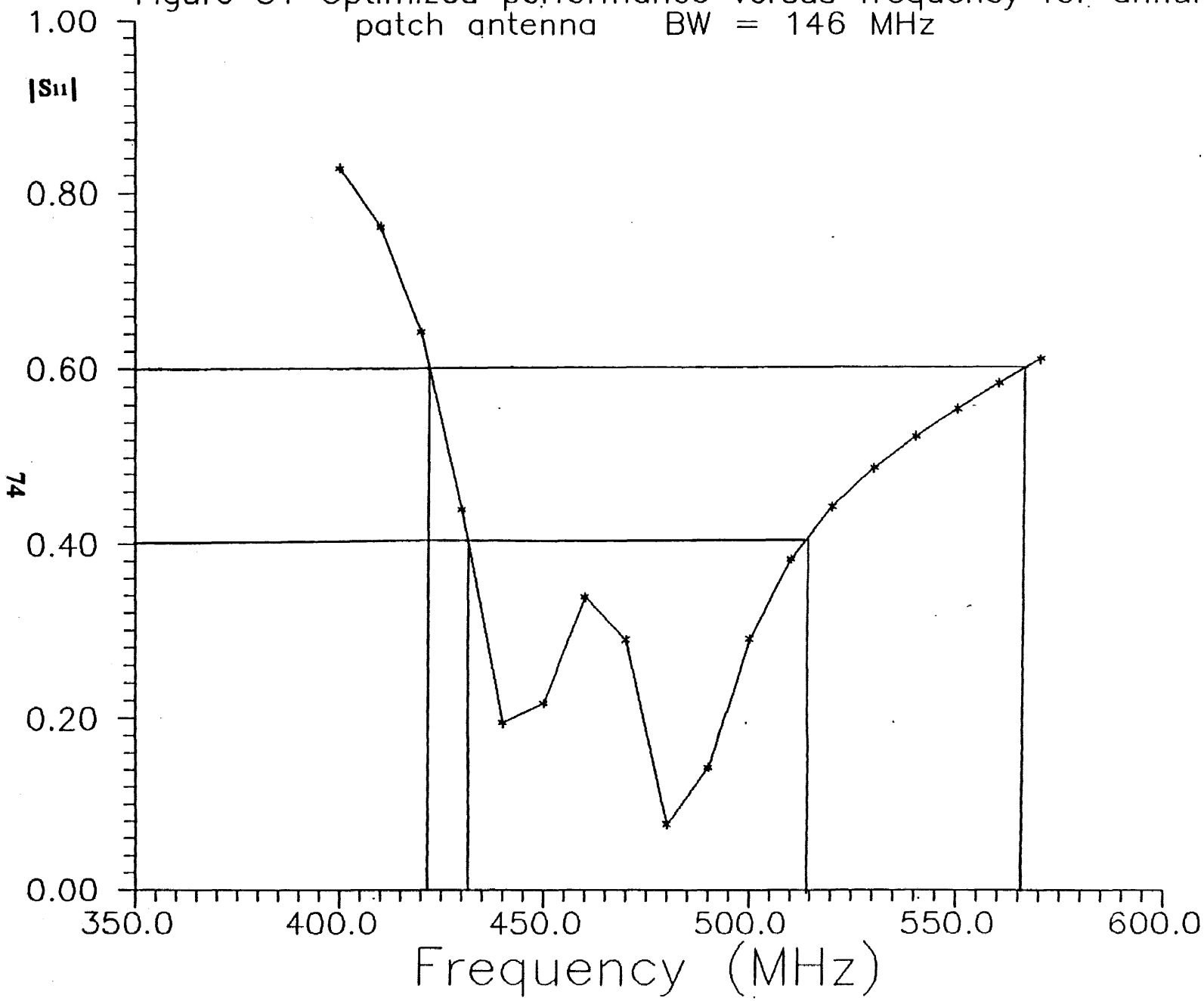

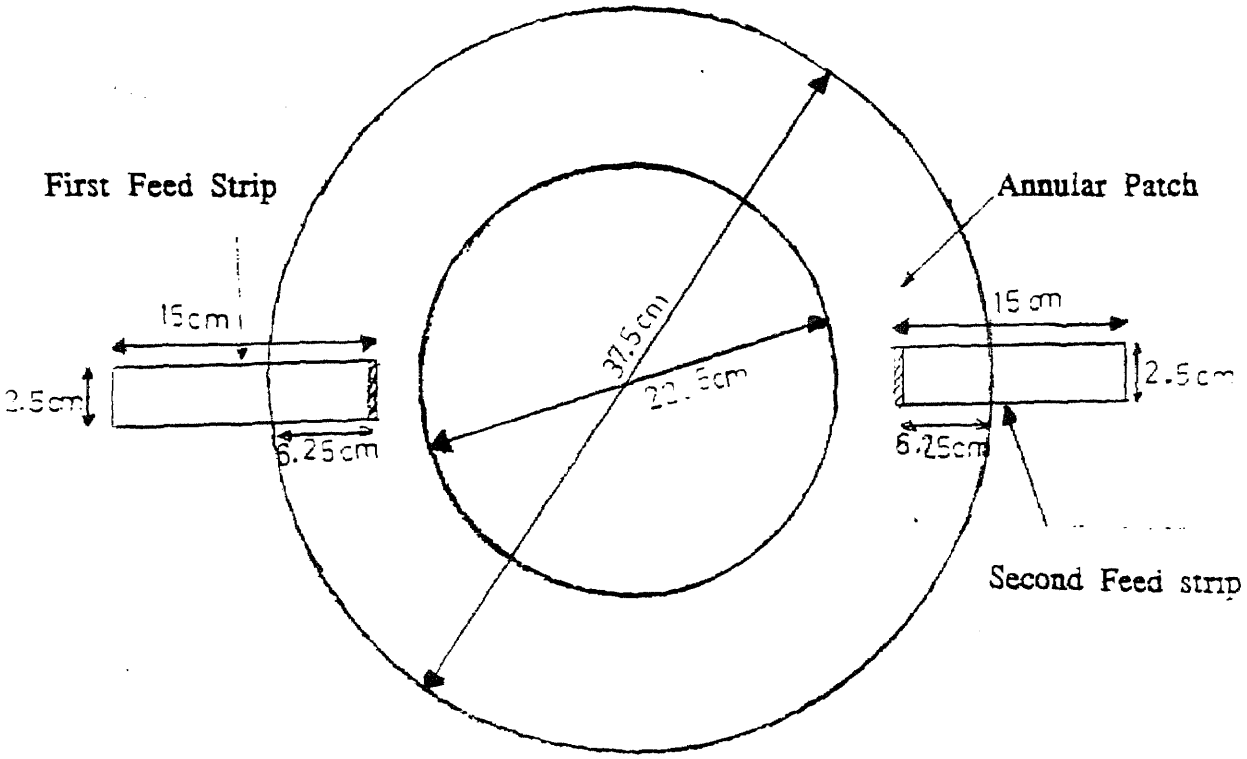

a) Patch geometry

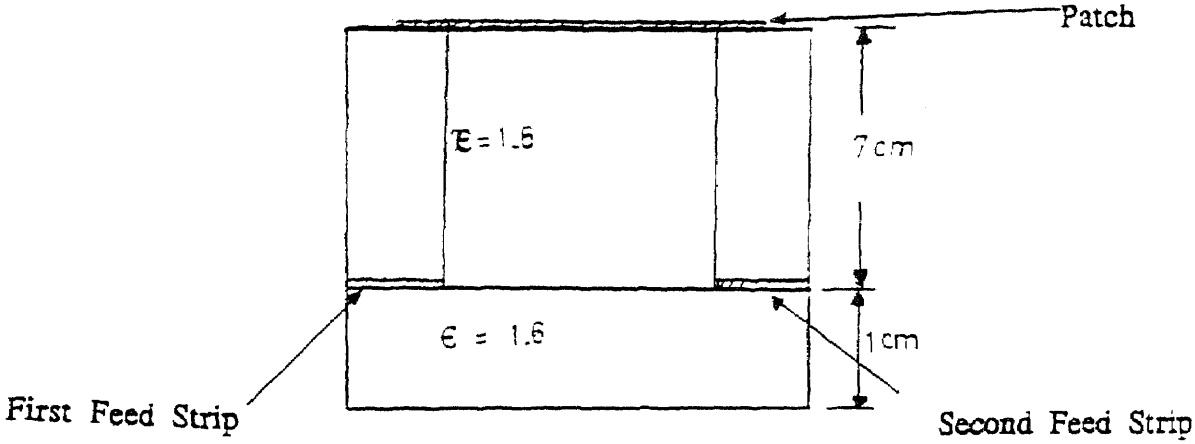

b) Crossectional view

Figure 52. Annular patch antenna with

double feed structure

Figure 53 Percentage of radiated power for the double feed annular ring patch antenna

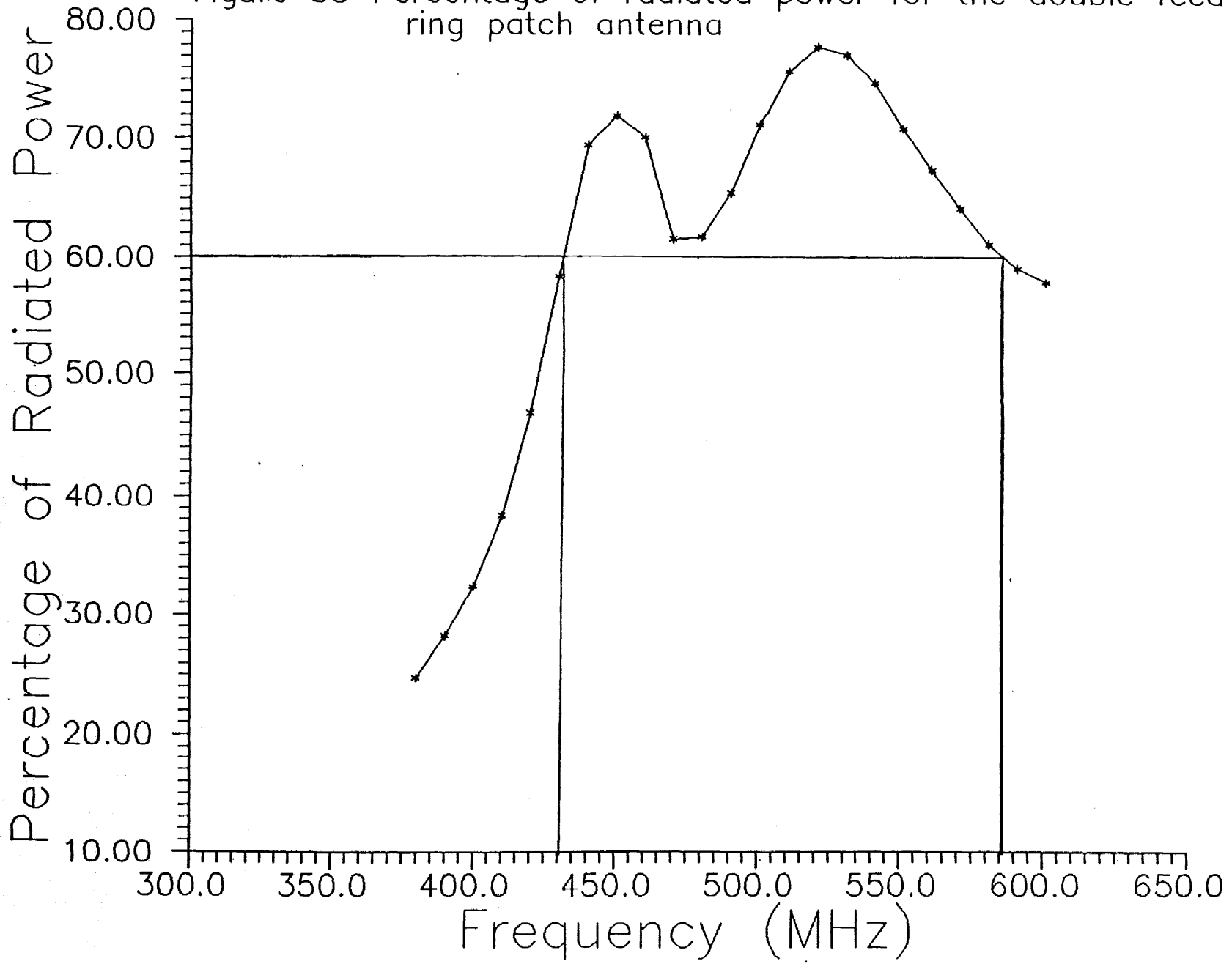

Chapter VI

CONCLUSIONS AND FURTHER WORK

Microstrip antennas traditionally exhibit narrow bandwidth performance characteristics. Increase in substrate thickness and modification of typical geometries are possible alternatives to achieve wideband radiation performance. In this work, a microstrip antenna is investigated which would fit into a typical size briefcase for a one man satellite link application. The available commercial software package developed by Sonnet Software Inc. is used to determine scattering parameters at the user defined antenna input ports. This computer code is validated by comparing its results with other numerical and experimental data for the rectangular patch antenna reported in the open literature. The proposed annular ring patch antenna geometry is optimized with respect to substrate thickness and feed location to obtain the desired bandwidth characteristics. The preliminary results obtained in this thesis indicate that it is possible to design an annular ring patch antenna which would yield more than 80 MHz bandwidth in the 400-500 MHz band.

However, further investigations have to be carried out to determine the circularly polarized nature of the radiated field, gain, radiation pattern and other parameters that cannot be obtained with the available software. Additionally, an antenna has to be fabricated and tested experimentally to validate the conclusion made in this thesis.

APPENDIX A

The input parameters for the geometry shown in Figure 13 involve the dielectric constant (ε_r) and the thickness of substrate to be 62 mils, the substrate dimensions of 1300 mils $\times$ 1080 mils and a cell size of 50 $\times$ 45 mils. The control input file was specified as shown below

```
----------------------
VER 2.0
GHZ
FRE 6.00   8.00    0.2
----------------------
```

where the first line indicates the running package version, the second line specifies the frequency units and the third line is to input the start frequency, the stop frequency and the step size.

The Circuit Response File generated by EM is shown below, where it includes the file name, the date and time it was run, the package version, box dimensions and all remaining specifications. It also shows the output results as three columns, Frequency, S-parameter magnitude and the Phase shift.

```
! ************************************************
! em -v antenna3.geo  -- Tue Dec  4 12:53:21 1990
! Em version 2.0, SN A1-142.
!  At least 20 subsections/wavelength.
! All dimensions are in mils.
A = 1300.00000(26), B = 1080.00000(24), C = 1062.00000, with 2 layers.
!  Layer  H( mils)      Erel    tan(d)     Murel    tan(d)  subs
!     0    1000.000  1.000000       0.0  1.000000       0.0  98
!     1    62.00000  2.220000       0.0  1.000000       0.0  0
! Metalization Losses (Ohms/square)
!   Top Cover    -- 377(DC),0*sqrt(F) - j 0 (DC)
! Circuit and excitation are symmetric about X axis.
! S-Parameters, Magnitude/Angle, Matrix order, Normalized to 50 Ohms.
# GHZ S MA
6.00000000 0.982815 0.7618
6.20000000 0.976009 -5.989
6.40000000 0.965702 -13.09
6.60000000 0.949720 -20.72
6.80000000 0.924057 -29.15
7.00000000 0.878731 -38.87
7.20000000 0.775894 -49.70
7.40000000 0.663721 -51.81
7.60000000 0.655984 -59.68
7.80000000 0.594003 -74.07
8.00000000 0.486753 -95.15
```

References

[1] Alexopoulous, N., P. Katehi, and D. Rutledge. "Substrate Optimization for Integrated Circuit Antennas," IEEE Trans. on MTT, Vol. MTT-31, No 7, pp.550-557, 1983.

[2] Bahl,I.and P. Bhartia, "Microstrip Antennas," Arteck House Inc., Dedham, Massachusetts, 1980.

[3] "Em User's manual," Sonnet Software Inc., 4397 Luna Course, Liverpool, New York 13090, July 15, 1990.

[4] James, J., P. Hall, and C. Wood, "Microstrip Antennas Theory and Design," IEE Publications, 1981.

[5] Miller, E. "Computational ElectromagneticsFrom a User's Perespective," AP Symposium Digest, Vol. 4, pp. 1493-1496, 1990.

[6] Munson, R., "Conformal Microstrip Antennas and Microstrip Phased Arrays," IEEE Trans. on Antenna and Prop., Vol. AP-22, pp. 74-78, 1974.

[7] Richards, W., "Microstrip Antennas," Antenna Handbook, Van Nostrand Reinhold Company Inc., New York, pp. 10-1 - 10-74, 1988.

[8] Sultan, M., "Extended Analysis of Closed-Ring Microstrip Antenna," IEE Proceedings, Vol. 136, Pt.H, No.1, pp. 67-69, 1989.

[9] Tomar, R., G. Gajda, K. Nguyen and E. Kpodzo, "Use of Touchstone in The Design and Analysis of Microstrip antennas," Bolrite Technologies, Inc., 150 Mill St., Carleton Place Ontario, Canada K7C 3P3.

[10] "Xgeom Users Manual," Sonnet Software Inc., 4397 Luna Course, Liverpool, New York 13090, July 15, 1990.